Chapter One

Introduction and basic concepts

1.1 Introduction:

From 1960 onwards, the increasing availability of intense,monochromatic laser sources provided a tremendous impetus to a wide range of spectroscopic investigations. The most immediately obvious application of early, essentially non-tunable, lasers was to all types of Raman spectroscopy in the gas, liquid or solid phase(Hollas, J.M., 2004).

Laser radiation is very much more intense, and the linewidth much smaller, than that from, for example, a mercury arc, which was commonly used as a spectroscopic source before 1960. As a result, weaker spectral intensity can now be observed and higher resolution is obtainable. In addition to carrying out conventional Raman experiments with laser sources new kinds of spectroscopy experiments became possible using Q-switched, giant pulse lasers to investigate effects which arise from the non-linear relationship between the induced electric dipole and the oscillating electric field.

For the branches of laser spectroscopy, most laser sources may appear to have a great disadvantage, that of non-tunability. In regions of the spectrum, particularly the infrared where tunable lasers are not readily available, ways have been devised for tuning, that is, shifting, the atomic or molecular energy levels concerned until the transition being studied moves into coincidence with the laser radiation. This may be achieved by applying an electric field to the sample, and the technique is called laser Stark spectroscopy. The corresponding technique using a magnetic field is that of laser magnetic resonance (or laser Zeeman) spectroscopy.

A useful way of changing the wavelength of some lasers, for example the CO_2 infrared laser, is to use isotopically substituted material in which the wavelengths of laser transitions are appreciably altered(Karl F. Renk, 2011).

In regions of the spectrum where a tunable laser is available it may be possible to use it to obtain an absorption spectrum. This technique can be used with a diode laser to produce an infrared absorption spectrum. When electronic transitions are being studied, greater sensitivity is usually achieved by monitoring secondary processes which follow, and are directly related to, the absorption which has occurred. Such processes include fluorescence, dissociation, or predissociation, and, following the absorption of one or more additional photons, ionization. The spectrum resulting from monitoring these processes usually resembles the absorption spectrum very closely.It may be apparent that, when lasers are used as spectroscopic sources, one can no longer think in terms of generally applicable experimental methods. A wide variety of ingenious techniques have been devised using laser sources. Laser spectroscopy has a great contribution to the discovery of the hundreds of lasers nowadays, and this allowed the field to be expanding very rapidly and involve a very large number of fields (Wolfgang Demtröder, 2008).Radiation from lasers is different from conventional light because, like microwave radiation, it is approximately monochromatic. Although each laser has its own fine spectral distribution and noise properties, the electric and magnetic fields from lasers are considered to have precise phase and amplitude variations in the first-order approximation. Like microwaves, electromagnetic radiation with a precise phase and amplitude is described most accurately by Maxwell's wave equations. For analysis of optical fields in structures such as optical waveguides and single-mode fibers, Maxwell's vector wave equations with

appropriate boundary conditions are used. Such analyses are important and necessary for applications in which we need to know the detailed characteristics of the vector fields known as the modes of these structures(N.G. Basov and O.N. Krokhin, 2006).

1.2 The study objectives:

The objectives of this research work are to identify the heavy metals in water samples, collected from different water sources in Khartoum State using laser induced breakdown spectroscopy (LIBS) technique.

1.3 The thesis structure:

Chapter one deals with an overview of laser spectroscopy and the objectives of this work. In chapter two, descriptions of Laser Induced Breakdown Spectroscopy, principles, capabilities, instrumentation and literature review are presented. Experimental setup, components of LIBS setup, samples collection and preparation procedure are presented in chapter three. In chapter four, results and discussion beside the conclusions and recommendations are reviewed.

1.4 Absorption and emission radiation:

Consider two energy levels, 1 and 2, of some atom or molecule of a given material with energies E_1 and E_2 ($E_1 < E_2$), respectively as shown in figure (1-1).The two levels can be any two of an atom's infinite set of levels. It is convenient however to take level 1 as the ground level(OrazioSvelto and David C. Hanna, 1998).

1.4.1 Absorption:

If the atom is initially lying in level 1 which is the ground level (Fig. 1.1c), the atom remains in this level unless some external stimulus is applied. That if EM wave of frequency $\upsilon = \upsilon_0$ is incident on the material. In this case there

is a finite probability that the atom will be raised to level 2. This is the absorption process (Franz Mayinger, 1994).

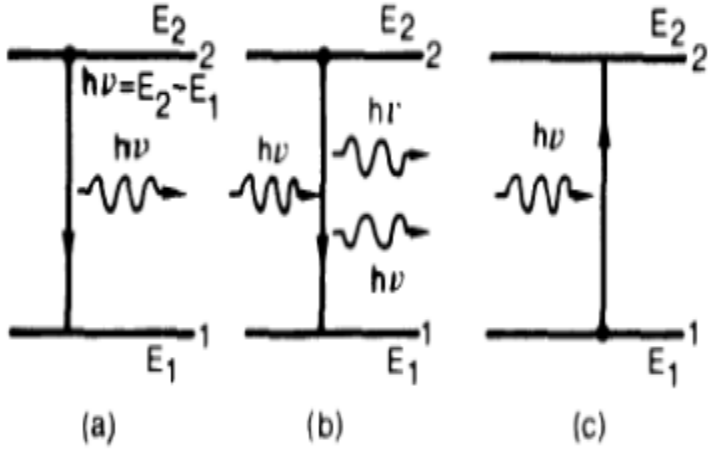

Figure (1-1) Schematic illustration of the three processes:
(a) spontaneous emission, (b) stimulated emission, (c) absorption.

The probability per unit time that it will absorb a quantum of radiation and raised to upper state (2) is proportional to the number of particles N_1 in the state 1 and the density of radiation ρ (ν).

The rate of absorption is equal

$$B_{12}N_1 \rho (\nu) \qquad (1\text{-}1)$$

Where B_{12} is proportionality constant named Einstein's coefficient of absorption (Wolfgang ,Demtröder, 2008).

1.4.2 Spontaneous emission:

Assume that the atom is initially at level 2. Since $E_2 > E_1$, the atom tends to decay to level 1. The corresponding energy difference E_2 — E_1 must therefore be released by the atom. When this energy is delivered in the form of an electromagnetic EM wave, the process is called spontaneous (or radiative) emission. The frequency υ_0 of the radiated wave is then given by:

$$v_0 = \frac{(E_2 - E_1)}{h} \qquad (1\text{-}2)$$

Where h is Planck's constant.

Spontaneous emission is characterized by the emission of a photon of energy $hv_0 = E_2 - E_1$ when the atom decays from level 2 to level 1 as shown in (Fig. 1.1a). The probability of spontaneous emission is proportional to the number of particles in the upper state, N_2. So the rate of spontaneous emission =

$$\mathbf{A_{21}N_2} \qquad (1\text{-}3)$$

Where A_{21} is the Einstein's coefficient of spontaneous emission

1.4.3 Stimulated emission:

If the atom is initially found in level 2 and an EM wave of frequency $\upsilon = \upsilon_0$ (i.e., equal to that of the spontaneously emitted wave) is incident on the material (Fig. 1.1b). Since this wave has the same frequency as the atomic frequency, there is a finite probability that this wave will force the atom to undergo the transition 2—1. In this case the energy difference $E_2 - E_1$ is delivered in the form of an EM wave that adds to the incident wave. This is the phenomenon of stimulated emission.There is a fundamental difference between the spontaneous and stimulated emission processes. In the case of spontaneous emission, atoms emit an EM wave that has no definite phase relation to that emitted by another atom. Furthermore the wave can be emitted in any direction. In the case of stimulated emission, since the process is forced by the incident EM wave, the emission of any atom adds in phase to that of the incoming wave and in the same direction(Milonni, P.W., andEberly, J.H., 2010).The rate of stimulated emission is proportional to the number of particles in the upper state, N_2 and the radiation density $\rho(\nu)$.

Rate of stimulated emission is equal

$$B_{21}N_2\rho(\nu) \qquad (1\text{-}4)$$

Where B_{21} is Einstein's coefficient of stimulated emission.

1.5 Laser in spectroscopy:

The use of laser in spectroscopy offered many advantages over light sources. Several important advantages over conventional spectroscopy with a broad-band background source and spectrometer like:

1. Higher spectral resolutions are usually attainable with a laser.
2. The low divergence makes it relatively easy to use long absorption path.
3. The high photon flux populates the upper level or the transition .3 soefficiently that absorption can be detected by the subsequent fluorescence even when the transition is weak.

The most commonly employed lasers for spectroscopic applications are tunable dye lasers and tunable solid state lasers. The CO_2 laser which offers line tuning over the range 9-11 μm has been employed in far infrared applications such as gas analysis and identification of chemical structures.

Even lasers that strictly are not tunable have been used, especially for some of the more exotic types of spectroscopy, like Raman spectroscopy. The argon laser has been used both its various fundamental wavelengths and a frequency-doubled with output in the UV. The Nd: YAG laser as a frequency-doubled, tripled and quadrupled device offers several useful wavelengths, especially in the UV (Milonni, P.W., andEberly, J.H., 2010). This ultraviolet and visible spectroscopy is extensively used for quantitative analysis of atoms, ions and chemical species in solution. Laser spectroscopy has many types such as:

1.5.1 Absorption spectroscopy:

Absorption spectroscopy is the study of the attenuation of the electromagnetic radiation by matter in which a photon is absorbed by a particle.It is probably one of the most widely used analytical tools in physics, chemistry, and industry.

There are two common ways used of laser-absorption spectroscopy,direct transmission measurements and opto-acoustic measurements, both methods are shown in figure (1-2) (HalinaAbramczyk, 2005).

,mm

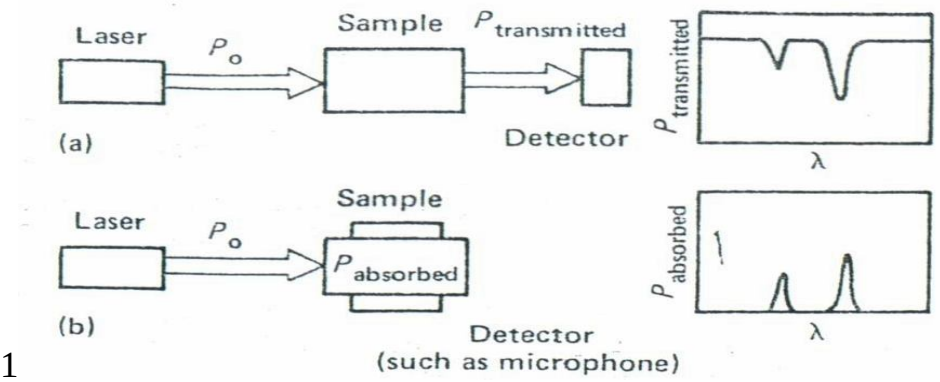

1

Figure (1-2): Linear laser-absorption spectroscopy using tunable laser

(a) Direct absorption. (b) opto-acoustic method using a microphone.

For absorption measurements, a tunable laser is used to scan over a range of frequencies. The intensity of the light exciting the measuring volume is recorded. Whenever the energy of one photon of the laser light is equal to the difference between two energy levels of the species in the measuring volume, the molecules absorb considerable amounts of the laser light and the intensity measured at the exit of the measuring volume decrease. The higher the density of the molecules,the more energy

isabsorbed, the higher temperature, the more transitions from higher initial energy levels are recorded.

There are many applications for absorption spectroscopy such as:

1.5.2 Laser-Induced Molecular Dissociation:

Many research groups have investigated possible application of laser photochemistry. The large majority of these researches have been done on laser isotope separation (LIS) and molecules dissociation.

Molecular dissociation falls into three categories:

- Can be induced by absorption of many photons from an infrared laser pulse and this is called infrared multiple-photon dissociation (IRMPD).
- By ultraviolet photolysis (UV), where this can be induced by excitation of molecule with a single (UV) photon.
- By infrared ultraviolet dissociation (IR-UV), where the absorption of one or more photons from the I.R produces some initial excitation, then the molecule dissociates by absorption of an ultraviolet photon.

Figure (1-3) gives a simple schematic representation of the three processes for a typical polyatomic molecule. The first of these, molecular dissociation induced by absorption of many photons from an infrared laser pulse. The second, UV, is dissociation induced by single ultraviolet photon. The third, IR–UV is a combination of these two arrows(OrazioSvelto, 2010).

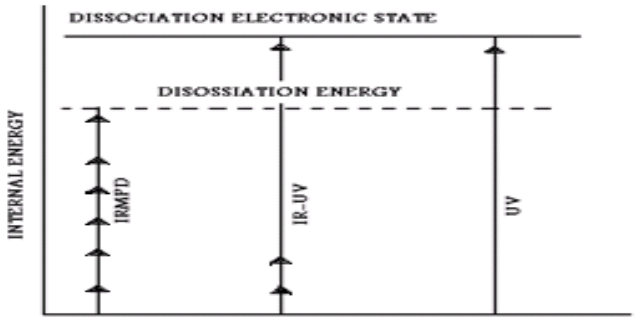

Figure (1-3): Schematic representation of laser photolysis by three methods.

The short arrows represent infrared photons and the long represent one ultraviolet photons.

1.5.3 Laser-Raman spectroscopy:

The Raman Effect is a spectroscopic technique used to study vibrational, rotational, and other low-frequency modes in a system.It relies on inelastic scattering, or Raman scattering, of monochromatic light, usually from a laser in the visible, near infrared, or near ultraviolet range(Christof Schulz, Volker Sick, 2004).The laser light interacts with molecular vibrations, phonons or other excitations in the system, resulting in the energy of the laser photons being shifted up or down. The shift in energy gives information about the phonon modes in the system

When the emitted photon is of lower frequency than the absorbed photon the process is termed stokes scattering.If the emitted photon is of higher frequency the process called anti-stokes scattering (the light has gained energy from vibrational or rotational state). These two processes are schematically represented in the energy diagrams shown in figure (1-4).

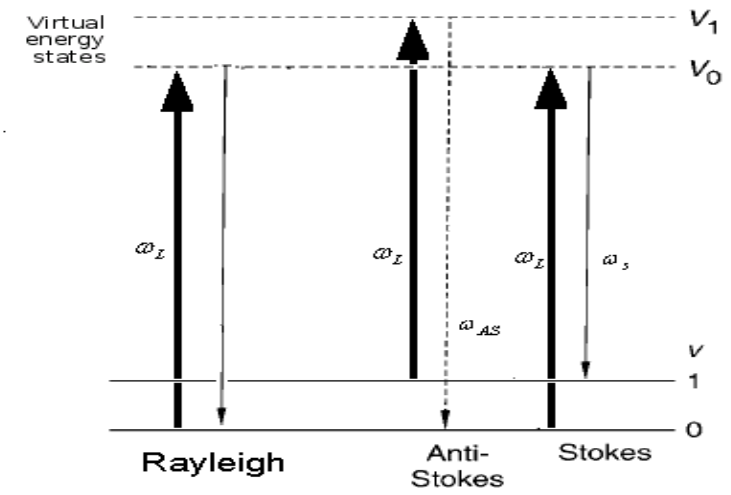

Figure (1-4): Energy-level diagram for spontaneous Raman scattering.

The bold arrows indicate the excitation photons at frequency ω_L, while the thin arrows represent the in elastically scattered photon, at frequency ω_s or ω_{AS}. Raman spectroscopy is carried out using visible or near UV excitation frequencies.The characteristics of the Raman signal yield a signature dependent on the molecular species, the temperature, and the pressure.

1.5.4 Hyper Raman spectroscopy:

Hyper Raman scattering is at a wavenumber $2\upsilon_0 \pm \upsilon_{HR}$ where υ_0 is the wavenumber of the exciting radiation and $-\upsilon_{HR}$ and $+\upsilon_{HR}$ are the Stokes and anti-Stokes hyper Raman displacements, respectively. The hyper Raman scattering is well separated from the Raman scattering, which is centered on υ_0, but is extremely weak, even with a Q-switched laser (J. Michael Hollas, 2004).

Scattering of wavenumber $2\upsilon_0$ is called hyper Rayleigh scattering, by analogy with Rayleigh scattering of wavenumber υ_0. However, whereas Rayleigh scattering always occurs, hyper Rayleigh scattering occurs only if

the scattering material does not have a center of inversion. Frequency doubled radiation consists of hyper Rayleigh scattering from a pure crystal. Consequently, one of the necessary properties of the crystals used, such as ADP and KDP, is that the unit cell does not have a center of inversion. Figure (1-5) shows the hyper Raman spectrum of gaseous ethane, C_2H_6, which belongs to the D_{3d} point group that has a center of inversion and therefore there is no hyper Rayleigh scattering at $2\upsilon_0$. In the hyper Raman spectrum a_{1u}, a_{2u} and e_u vibrations are allowed. None of these is allowed in the normal Raman spectroscopy.

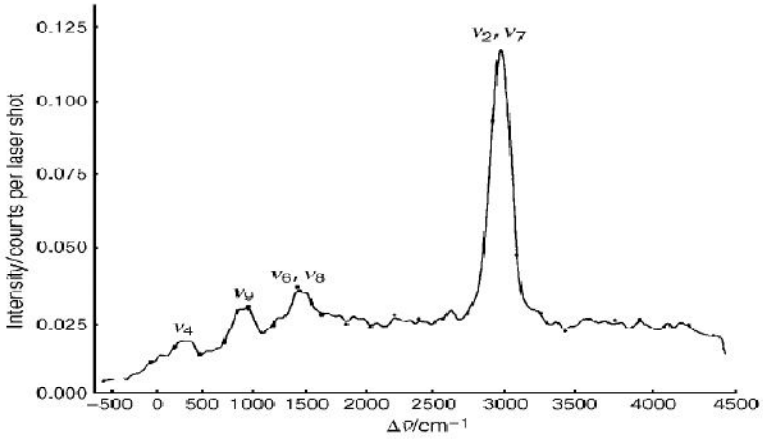

Figure (1-5)the hyper Raman spectrum of ethane.

1.5.5 Stimulated Raman spectroscopy:

Stimulated Raman spectroscopy is experimentally different from normal Raman spectroscopy in that the scattering is observed in the forward direction, emerging from the sample in the same direction as that of the emerging exciting radiation, or at a very small angle to it as shown in Figure (1-6).The stimulated Raman scattering can be observed by focusing radiation from a Q-switched ruby laser with a lens L into a cell C containing, the sample.

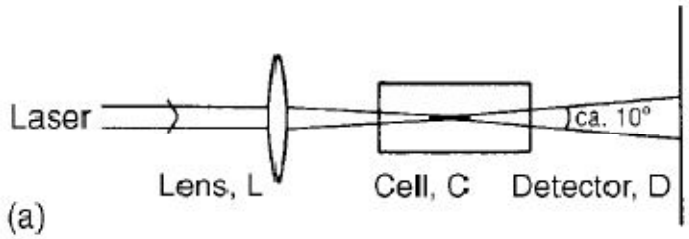

Figure (1-6) Stimulated Raman scattering experiment.

The forward scattering, within an angle of about 10^{o}, is collected by the detector D. If the detector is a photographic color film, broad concentric colored rings ranging from dark red in the center to green on the outside are observed, as shown in Figure (1-7) (Zhang, S., et.al 2005).

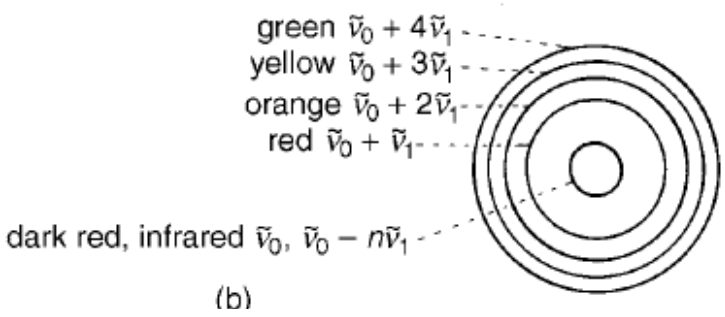

Figure (1-7) concentric rings observed, in the forward direction.

1.5.6 Coherent anti-Stokes Raman scattering spectroscopy:

Coherent anti-Stokes Raman scattering, or CARS as it is usually depends on the general phenomenon of wave mixing, as occurs, for example, in a frequency doubling crystal in case three-wave mixing occurs involving two incident waves of wavenumber υ and the outgoing wave of wavenumber 2υ.

In CARS, radiation from two lasers of wavenumbers υ_1 and υ_2, where $\upsilon_1 > \upsilon_2$, fall on the sample. As a result of four-wave mixing, radiation of wavenumber υ_3 is produced there. The scattered radiation υ_3 is to high

wavenumber of υ_1 (on the anti-Stokes side) and is coherent, unlike spontaneous Raman scattering

$$\tilde{\nu}_3 = 2\tilde{\nu}_1 - \tilde{\nu}_2 = \tilde{\nu}_1 + (\tilde{\nu}_1 - \tilde{\nu}_2) \quad (1\text{-}5)$$

1.5.7 Laser induced fluorescence:

Laser induced fluorescence (LIF) is emitted from electronically excited levels that are populated by absorption of photons, typically in the ultraviolet and visible spectral region (David A. Cremers, Leon J. Radziemski, 2006).

In this technique the laser beam is formed into a thin light sheet by a set of lenses, and this light sheet entering the observation volume. The fluorescence is captured by a collecting lens and imaged on to the detector surface. The data of the image is transferred from the camera to the control unit installed in a computer.

The emitted radiation is characteristic for the concentration and temperature of the regarded species.

1.5.8 Cavity ring-down spectroscopy:

If radiation of a particular wavelength λ, or wavenumber ν, of intensity I_0 enters a cell of length L, containing an absorbing sample, and emerges from the cell with reduced intensity I, the absorbance A is given by:

$$A = \log_{10}(I_0/I) = \varepsilon(\tilde{\nu})c\ell \quad (1\text{-}6)$$

$$I/I_0 = \exp(-\alpha c t_\ell) \quad (1\text{-}7)$$

The experimental method used for CRDS is illustrated in Figure (1-11) (Wang, C.Y. and Huang, Z., 2009).

Radiation from a pulsed laser enters the cavityformed between two mirrors M_1 and M_2.These mirrors are Plano concave, with flat outer and concave inner surfaces, coated on the inner surfaces with a material which is very highly reflecting at the wavelength being employed. A reflectivity as high as 99.93% has been recorded at 515 nm but this decreases with wavelength. Consequently, when a photon enters the cavity, it may be reflected backwards and forwards many times between the mirrors before it emerges to the detector.

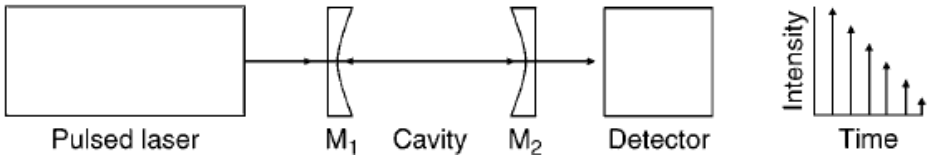

Figure (1-8) Schematic diagram showing how a cavity ring-down absorption spectrum is obtained.

In the near infrared it is not unusual for it to be reflected 5 000 times so that, with a cavity length of 1 m, the effective Absorption path length is 10 km. Such large path lengths, obtainable in a relatively compact space, make CRDS an extremely sensitive and convenient technique for detection of very weak absorption. This may be weak because the transitions being studied have a very low probability or because the molecule being studied is present in only very low concentration.

At longer times, after more traversals, the signal decreases: Equation (1-7) illustrate that the rate of decrease due to absorption is exponential. Measurement of this rate of decrease gives a very accurate value of the linear absorption coefficient α. The variation of α, as the wavelength of the laser is tuned through the region in which the sample absorbs, gives the absorption spectrum.

1.5.9 Light detection and ranging (LIDAR):

LIDAR works in a similar way that radar work except the source of radiation is a pulsed laser and the wavelength lies in the infrared, visible or ultraviolet region. It also used as a tool for spectroscopic measurements on various gases present in the atmosphere. Figure (1-9) shows a typical LIDAR device. Radiation from the laser, in the form of a highly parallel beam, is reflected by the mirror M_1 and directed to the part of atmosphere being investigated(HalinaAbramczyk , 2005).

The choice of the return time for the backscattered laser pulse is a consequence of the choice of height in the atmosphere at which measurements are required. The device commonly used for collecting the backscattered light is a Cassagrain telescope consisting of a large concave mirror M_2, which collects the radiation, and a further mirror M_3 which reflects and focuses it onto the detector.

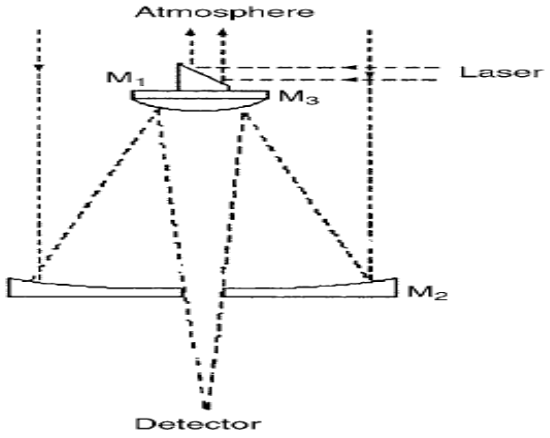

Figure (1-9)A LIDAR device using a Cassagrain telescope.

Determination of the concentration, and height distribution, such as of ozone or any molecular atmospheric pollutant is carried out using the DIAL (differential absorption LIDAR) technique. For a molecule such as carbon dioxide which shows sharp, discrete absorption, the gas concentration at a

particular height (using a particular time delay for the returned, backscattered laser radiation) is obtained by comparing the intensity of the backscattered laser beam with the laser wavelength tuned onto and then off an absorption feature of the molecule being investigated. Any background absorption and backscatter by, for example, an aerosol which may be present in addition to the gas of interest is taken account of by comparison with the intensity of the returning laser beam when the wavelength is on and off a sharp absorption feature.

1.5.10 Femtosecond spectroscopy:

Femtosecond lasers can be used for the direct investigation of extremely fast processes occurring on a time scale of a few picoseconds or less. An example of such a physical process is molecular vibration, a typical vibration occurring on a time scale of 0.1–1.0 ps. also fast chemical processes which occur on a picosecond time scale are the transfer of an electron during a reaction or the breaking of a bond in dissociation(David A. Cremers, Leon J. Radziemski, 2006). When a chemical bond is broken by photolysis, following the absorption of a quantum of radiation of appropriate energy, there is a smooth change from the bound molecule to the products. For example, the molecule AB may dissociate into A+ B, where the A and B are atomic or molecular fragments. The smooth change from reactant to products involves the so-called transition state A·····B in which the bond between A and B is weakened as they move apart. Before it became possible to use femtosecond lasers to investigate the structure of such transition states the only means of doing so were indirect.

One method involves the use of two intersecting molecular beams, one containing A and the other B, which react to produce AB at the point of intersection. Structure of the transition state may be infrared by changing the states (rotational, vibrational or electronic) of A and/or B. A second method of obtaining evidence regarding the structure of the transition state is to dissociate AB and investigate the energy states of one or both of the products by, for example, laser induced fluorescence, photocoustic spectroscopy.

CHAPTER TWO

Laser Induced Breakdown Spectroscopy, Principles and Applications

2.1 Introduction:

Laser-induced breakdown spectroscopy (LIBS) is a method of atomic emission spectroscopy (AES) that uses laser-generated plasma as the hot vaporization, atomization, and excitation source (Hammer, S.M., et.al, 2006). Because the plasma is formed by focused optical radiation, the method has many advantages over conventional AES techniques that use an adjacent physical device (e.g. electrodes, coils) to form the vaporization/excitation source. Foremost of these is the ability to interrogate samples in situ and remotely without any preparation. In its basic form, a LIBS measurement is carried out by forming laser plasma on or in the sample and then collecting and spectrally analyzing the plasma light. LIBS as most commonly used and shown schematically in Figure (2-1).Qualitative and quantitative analyses are carried out by monitoring emission lines positions and intensities. Although the LIBS method has been in existence for 40 years, prior to 1980, interest in it centered mainly on the basic physics of plasma formation. Since then the analytical capabilities have become more evident (Hammer, S.M., et.al, 2006).

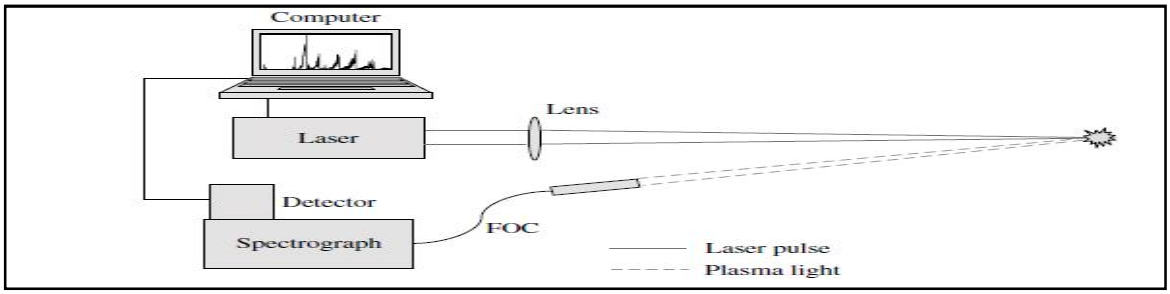

Figure (2-1): the conventional LIBS system configuration.

2.2 Fundamentals of LIBS:

2.2.1 Introduction:

As previously mentioned, LIBS is a form of atomic emission spectroscopy AES, a broad category of analysis tools that rely on the unique optical features individual elements emit when decaying from an excited state (Cremers and Radziemski, 2006; Radziemski, 2002; Winefordner et al., 2004). In all forms of AES, an analyte is vaporized, atomized, and generally ionized, yielding a mix of neutral atoms, electrons and ions with which an energy source stimulates the resultant species to an unstable excited state. As excited species decay back to their ground states they emit light of a characteristic wavelength that can be used qualitatively to determine the elemental composition of the original sample, and when intensity is calibrated to molar concentration or mass the signal can also quantitatively resolve the initial analyte composition. In the LIBS technique specifically, a pulsed laser focused down to a small target volume causes the formation of a high-temperature (tens of 1000's of degrees) plasma and thereby acts as a single source for excitation as well as vaporization/atomization/ionization In this case, the early emission from the plasma is white light (i.e. broadband continuum) spectral radiation caused by the recombination of free electrons and ions along with bremsstrahlung radiation; however, over time the continuum emission fades allowing for individual atomic spectral features corresponding to constituent species to be discerned(Gilbarg, D. and Trudinger, N.S., 2015).

The only requirement of the laser itself is that it is capable of producing sufficient power during pulsed operation to generate the plasma itself; the most commonly used laser for this purpose is a solid state laser such as an

Nd: YAG (Lee et al., 1997). In order to achieve the necessary power, a lens is used to focus the laser beam down to a small volume in which plasma formation occurs. Emitted light is directed back toward some type of detection device, with options including a simple camera, photomultiplier tube (PMT), photodiode array (PDA), or charge transfer device such as a charge-coupled device (CCD) or intensive charged coupled device (ICCD). Because the LIBS signal is time variant, a gating mechanism is required to obtain a signal integrated over a specific length of time at an optimal delay interval (Demirbas, A., 2004).Like all forms of AES, LIBS presents advantages over chemical digestion forms of species analysis in that it can distinguish all elements and can detect multiple elements in the same sample simultaneously. In addition, LIBS goes beyond other AES techniques in that analysis is performed in real time with virtually no sample preparation (in many cases *in sit*u), it has high sensitivity, and is applicable to all phases of matter. Because of these unique advantages, LIBS has been applied over an ever widening range of applications, including hazardous emissions detection, environmental monitoring, sorting of industrial materials, and aerosol analysis (Radziemski, 2002). LIBS has even been used to clean historical documents while monitoring composition to ensure no damage to the underlying fibers (Kaminska et al., 2007). Despite the positives, however, LIBS is not a flawless technique, with one key concern being matrix effects the plasma may have on the emitted signal. Although for quantitative analysis of a given species the resultant signal must be independent of additional elements within the plasma, temperature, and so forth, this situation is not the case within all LIBS plasma and care must be taken to insure robust conditions. The nature of LIBS also presents a possible disadvantage when analyzing large samples; the focused laser

provides a point source analysis of the target's surface, therefore non-homogeneities within the bulk of the material may be difficult if not impossible to detect. We go over this point by putting the sample on a rotating platform. The point-source nature of LIBS becomes an advantage, however, in the case of aerosol analysis. Assuming complete vaporization of the target particle, sample non-homogeneities do not present a concern in this case, and quantitative analysis of particle ensembles as well as individual aerosol particles has been shown to be possible (Hahn and Lunden, 2000).

2.2.2 Plasma parameters:

Three fundamental parameters characterize the plasma:

1. The particles density n or electron density (measured in particles per cubic meter).
2. The temperature T of each species (usually measured in eV, where 1 eV=11,605 K), For a typical LIPS Laser Induced Plasma Spectroscopy, the electron temperature could be around 10,000 K.
3. The steady state magnetic field B (measured in Tesla).

A host of subsidiary parameters (e.g., Debye length, Larmor radius, plasma frequency, cyclotron frequency, thermal velocity) can be derived from these three fundamental parameters. For partially-ionized plasmas, the fractional ionization and cross-sections of neutrals are also important.

2.2.3 Fundamentals of absorption and emission:

Atomic absorption and emission require the prevalence of free atoms which, in most instances, is achieved in plasma or a plasma-like state. When plasma is contained in a closed system and is in thermal equilibrium, the population of the excited levels may be described for one species by Boltzmann's law:

$$\frac{N_q}{N_0} = \frac{g_q}{g_0} \exp(-Eq/kT) \quad (2\text{-}1)$$

With N_q: number of particles in the excited state, $N_{0:}$ number of particles in the ground state, $g_q$and $g_{0:}$ statistical weights of the corresponding energy levels; $E_{q:}$ excitation energy of the state *q; k:* Boltzmann's constant (= 1.38 $\times 10^{-23}$ J K^{-1}), and *T:* absolute temperature. When the plasma is in the steady state, the number of particles that leave an energy level per time unit is equal to that of those that arrive at this level. A number of phenomena are responsible for the transition of species between energy levels in plasma:

a) Collisions of atoms, leading to the excitation of one species to a higher energy level (collisions of the first kind).
b) Collisions of an excited species with another particle, leading to radiationless relaxation (collisions of the second kind).
c) Excitation by collision with electrons.
d) De-excitation with the transfer of energy to an electron.
e) Excitation of atoms or ions by the absorption of radiation.
f) de-excitation of atoms or ions by spontaneous or stimulated emission Assuming the presence of two species, with *n* being the concentration of one species and *N* that of the second species that is in large excess (*N* >>*n*), we can set up the following equations:

$$\alpha N n_0 = \beta\, N\, n_q \quad (2\text{-}2)$$

$$\alpha_e n_e\, n_0 = \beta_e\, n_e\, n_q \quad (2\text{-}3)$$

$$B' \rho_v n_0 = (A + B\rho_v) n_q \quad (2\text{-}4)$$

A, *B*, and B' are the Einstein transition probabilities for spontaneous emission, stimulated emission, and absorption, respectively; and α_e, α, β_e and β are the cross sections of the respective processes (which are also a function of the velocity distribution of the particles involved). n_e is the electron

density; ρ_v is the radiation density at a given frequency v(Bhatia, N.P., Szegö, G.P. and Szegö, G.P., 2002).

When the system is in thermodynamic equilibrium, the rate of formation and disappearance of charged particles and neutrals is equal, and at a given temperature T we can state:

$$\frac{n_q}{n_0} = \frac{\alpha}{\beta} = \frac{\alpha_e}{\beta_e} = \frac{B'}{A/\rho_v + B} = \frac{g_q}{g_0} \exp(-Eq/kT) \quad (2\text{-}5)$$

The number of charged and uncharged species remains constant through excitation and de-excitation by collisions with neutrals, ions and electrons. Absorption and emission, as they occur in a real radiation source, certainly also have to be considered, but they normally contribute only very little to the energy balance which is in the so-called local thermal equilibrium (LTE):

$$\alpha N n_0 + \alpha_e n_e n_0 + B' \rho_v n_0 = \beta N n_q + \beta_e n_e n_q + (A + B\rho_v) n_q \quad (2\text{-}6)$$

From Eq. (2-5), $nq/n0$ can be calculated. In the radiation source, the population of excited states is determined by the excitation process, as may be deduced from Eq. (2.6): Thus, for example, a d. c. arc source (that is said to be in LTE), $\alpha N >> (\alpha e n_e + B'\rho)$, and $\beta N >> [\beta e n_e + (A + B\rho_v) n_q]$ (Yu, L. and Andriola,A., 2010).

As long as the radiation density is low (which is the case for the d. c. arc) the plasma can be assumed to operate under local thermal equilibrium. This is not the case for low pressure discharges where both collisions with electrons and radiative de-excitation are very important. Also, for low-pressure plasmas, the assumption of a Maxwellian velocity distribution of the particles is no longer valid. Species can decay from excited states through a number of processes, including collision with uncharged (molecules, atoms) or charged (ions, electrons) particles, or by the emission

of electromagnetic radiation. In the case of radiative decay, the wavelength of emission is given by Planck's law. For the spontaneous decay from level *q* to level *p*, the number of events per unit time is:

$$\frac{\mathrm{d}\,N_q}{\mathrm{d}\,t} = A_{qp}\,N_q \qquad (2\text{-}7)$$

$A_{qp}$is the Einstein coefficient for spontaneous emission (s^{-1}). Equation (2-7) must be adapted when several transitions starting from level *q* are to be considered:

$$\frac{\mathrm{d}\,N_q}{\mathrm{d}\,t} = N_q \sum A_{qp} = N_{q\nu q} \quad (2.8)$$

$\upsilon_q$is here the lifetime of the excited state *q*. The typical lifetime of an excited state from which a species decays through an allowed radiative transition is of the order of 10^{-8} s. When radiative transitions are not allowed, the excited states are metastable (as is the case, e. g. for the Ar 11.5 and 11.7 eV states), and relaxation can only occur through collisions with other particles. Absorption of electromagnetic radiation of frequency $\upsilon_{qp}$and radiation density $\rho_\upsilon$increases the number density of excited particles *Nq*to:

$$\frac{\mathrm{d}\,N_q}{\mathrm{d}\,t} = \mathrm{B'_{qp}}\,N_0\,\rho_\nu \qquad (2\text{-}9)$$

Stimulated emission takes place when atoms in the excited state *q* decay upon interaction with radiation of wavelength $\lambda qp$and leads to a reduction in the number density of excited species according to:

$$\frac{\mathrm{d}\,N_q}{\mathrm{d}\,t} = \mathrm{B_{qp}}\,N_q\,\rho_\nu \quad (2\text{-}10)$$

Under conditions of thermal equilibrium:

$$g_q B_{qp} = g_p B_{pq} \quad (2\text{-}11)$$

Where g_q and g_p are the statistical weights (degeneration factors) of levels *p* and *q*. When species emit, the intensity of the emitted spectral line (denoted

by the subscript *a*) is proportional to the number density of atoms in the excited state *q*:

$$I_{qp} = A_{qp} n_{aq} h \upsilon_{qp} \qquad (2\text{-}12)$$

n_{aq}may be substituted using the Boltzmann equation:

$$I_{qp} = A_{qp} h \upsilon_{qp} n_a \frac{g_q}{Z_a} \exp(-Eq/kT) \qquad (2\text{-}13)$$

The sum $Z_a = \sum_a g_a \exp(-E_q / kT)$ is the partition function. It is a function of temperature, and the coefficients of this function are tabulated in the literature for a large number of atoms and ions. When the intensities of two emission lines *a* and *b* from the same ionization state of an element are used, the excitation temperature *T* may be calculated from:

$$T = \frac{5040(E_a - E_b)}{\log[(g_a A_a)/(g_b A_b)] - \log(\lambda_a / \lambda_b) - \log(I_a / I_b)} \qquad (2\text{-}14)$$

In this equation, energies are in eV, and $E_a$and $E_b$denote the excitation energies (in eV) of lines *a* and*b*. The line pair Zn 307.206 nm/Zn 307.59 nm is very often used for calculating the excitation temperature. It is particularly suitable, as ionization of zinc is generally low (due to its high ionization energy), the difference between the two wavelengths is not too large, ensuring a uniform detector response, and the *gA* factors are precisely known.

2.2.4 Line broadening:

Due to the contribution of various broadening mechanisms, the line widths typically observed in atomic spectrometry are significantly broader than the natural width of a spectroscopic line which can be theoretically derived. The natural width of a spectral line is a consequence of the limited lifetime τ of

an excited state. Using Heisenberg's uncertainty relation, the corresponding half-width expressed as frequency is:

$$\Delta\nu_N = \frac{1}{2\pi\tau} \qquad (2\text{-}15)$$

From this equation, a typical half-width of Ca. 10^2 pm is obtained formost spectroscopic lines. The first important line broadening mechanism is Doppler line broadening. It results from the movement that emitting species make towards or away from the point of observation. The contribution to line broadening is:

$$\Delta\nu_D = 2\sqrt{\ln(2)c}\,\upsilon_0\sqrt{2RT/M} \qquad (2\text{-}16)$$

Where c is the velocity of light, υ_0 the frequency of the emission maximum, R the gas constant and M the atomic mass. Eq. (2-16) suggests that Doppler line broadening is strongly temperature dependent. It has therefore also often been termed temperature broadening. It may thus be used to determine the kinetic energy of the emitting atoms or ions. For example, Doppler broadening is about 0.8 nm for the Ca(I) 422.6 nm emission at 300 K and reduced pressure (0.1 kPa), while it approaches 2 pm at 3000 K. Pressureor Lorentz broadeningis the second important factor for line broadening. It is a result of the interaction of the emitting species and other, non-emitting particles. Its contribution to line broadening is:

$$\Delta\nu_L = (2/\pi)\sigma^2{}_L\, N\sqrt{2\pi RT\left(\frac{1}{M_1}+\frac{1}{M_2}\right)} \qquad (2\text{-}17)$$

Where M_1 and M_2 are the atomic masses of the two interacting species.

N is the concentration of the foreign atom species and L is its cross-section. At low pressure, the contribution of pressure broadening is low, e. g. for the Ca (I) 422.6 nm line only about 0.02 pm at 300 K and 0.9 kPa. However, with increasing pressure, this contribution becomes the dominant factor for

line broadening. Other factors contributing to line broadening are isotopic effectsand hyperfine structure(as a result of the interaction between radiating and non-radiating atoms of the same species) and Stark broadeningwhich are due to the interaction with electric fields.

2.3. LIBS Instrumentation:

Laser Induced Breakdown Spectroscopy (LIBS) is a widely exploited atomic emission spectroscopic technique suitably conceived for the analysis of the elemental composition of a large variety of materials (solid, liquid and gas samples (Singh, J.P. and Thakur, S.N. eds., 2007). Typical features, that have made this technique very popular, are: the absence of any preparation/treatment of the samples, the question destructive and micro-analytical character of the measurements, the capability of detecting in a single measurement both neutral and ion spectral features of all the atomic and molecular species present in the sample, the capability of performing stand-off measurements as well as the availability of simple, inexpensive and compact portable LIBS systems. Because of these quite unique characteristic features, the number of LIBS applications is greatly increased during the last years, giving rise to different experimental configurations properly designed to match the requirements stemming from the specific application. With an overview of the LIBS instrumental techniques so far utilized (at least the most important ones) by describing the optical and electronic components that are present in a LIBS system and how their technical characteristics as well as their specific configurations may affect LIBS measurements. In a LIBS measurement, a short laser pulse (typically ranging from the nanosecond to femtosecond time scale) is focused onto the sample to be analyzed. Since a fraction of the impinging energy is transferred to the matter, a high temperature and high electron density

plasmais formed in correspondence of the irradiated region (phenomenon usually referred to as breakdown). Different phenomena may contribute to the plasma ignition process, depending on both the excitation pulse physical characteristics (i.e. wavelength, duration, intensity, repetition rate, etc.) and the physical properties of the irradiated material. As a consequence of the plasma formation, a small amount of material is vaporized and expands at a supersonic velocity in a direction perpendicular to the target surface. Provided that the elemental composition of the plasma plume is the same as that of the target material (stoichiometric ablation).The electromagnetic radiation emitted by the plasma can be detected and spectrally analyzed to retrieve the local elemental composition of the sample. Attention, however, has to be paid to the temporal delay at which the emitted spectrum is recorded. In fact, at the beginning, the spectrum is in the form of broad emission lines (line broadening is mainly due to Stark effect) superimposed to an intense continuous background due to both the free–free electron transitions (Bremsstrahlung emission) and the free to bound electron recombination. After few hundreds of nanoseconds, however, free electrons are captured by ions so that the continuous background intensity decays quite rapidly while the atomic emission lines (due to bound to bound electronic transitions) become narrower and weaker. At longer delays (greater than 10 s) the atomic lines decay slowly while emissions from simple molecules start appearing. It is worth mentioning here that for applications where quantitative analysis is required, the acquisition time should be limited to a small fraction of the total plasma emission time, so to guarantee thermodynamic equilibrium conditions (Federer, H., 2014).A few instruments based on LIBS have been developed but have not found widespread use. Recently, however, there has been renewed interest in the

method for a wide range of applications. This has mainly been the result of significant technological developments in the components (lasers, spectrographs, detectors) used in LIBS instruments as well as emerging needs to perform measurements under conditions not feasible with conventional analytical techniques. A review of LIBS literature shows that the method has a detection sensitivity for many elements that is comparable to or exceeds that characteristic of other field-deployable methods (Federer, H., 2014).A typical LIBS apparatus is shown diagrammatically in Figure (2-2) along with a photo of a simple LIBS apparatus.

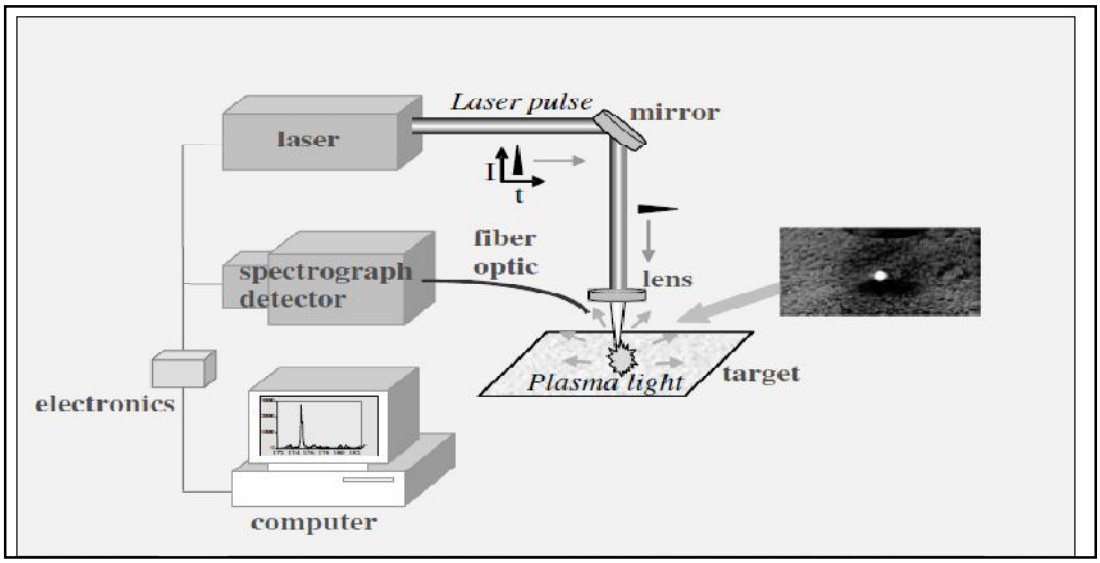

Figure (2-2): Schematic of typical experimental LIBS setup.

The main components are:

(1) The pulsed laser that generates the powerful optical pulses used to form the microplasma;

(2) The focusing system of mirror and lens that directs and focuses the laser pulse on the target sample;

(3) Target holder or container (if needed);

(4) The light collection system (lens, mirrors or fiber optic) that collects the spark light and transports the light to the detection system;

(5) Detection system consisting of a method to spectrally filter or disperse the light such as a spectrograph and a detector to record the light;
(6) Computer and electronics to gate the detector, fire the laser, and store the spectrum. The basic components of any LIBS system are similar but the component specifications are tailored to the particular application. These specifications include physical parameters such as size, weight, packaging, power and utilities required for operation as well as technical specifications pertaining to operational performance. These will be discussed in detail below, but examples include the energy of the laser pulse and the spectral resolution of the spectrograph (Radziemski, L.J., andCremers, D.A., 2006).

2.4.Lasers for LIBS:

Generally pulsed lasers are used in the production of plasmas and also in laser-induced breakdown spectroscopy (LIBS). We consider only those properties of lasers relevant to plasma production in gaseous, liquid and solid samples. It is possible to generate short duration laser pulses with wavelengths ranging from the infrared to the ultraviolet, with powers of the order of millions of watts. Several billions to trillions of watts and more have been obtained in a pulse from more sophisticated lasers. Such high-power pulses of laser radiation can vaporize metallic and refractory surfaces in a fraction of a second. It is to be noted that not only the peak power of the laser, but also the ability to deliver the energy to a specific location is of great importance. For LIBS, the power per unit area that can be delivered to the target is more important than the absolute value of the laser power. The power per unit area in the laser beam is termed “irradiance” Conventional light sources with kilowatts powers cannot be focused as well as laser radiation and therefore are not capable of producing effects that lasers can all rights reserved (Sirin et.al, Y, 2007).

2.5. Spectrographs:

Basic spectrographs there are different designs (or mountings for the grating) such as the Littrow, Ebert-Fastie, Czerny-Turner, Paschen-Runge, and crossed-Czerny-Turner. (Tsuji, J., 2006).

The design differences relate to whether one or two mirrors are used for collimating and focusing the light and the position of the slits relative to the grating. Isthe most common variant in use here, light from the plasma is imaged onto the entrance slit. The light passing through the slit reaches the first mirror which collimates the light, directing it on to the grating. Ideally the grating will be filled with the light reflected by the mirror to achieve maximum resolving power. Light is reflected off the grating at different angles according to wavelength. This light then strikes a second mirror that focuses the light, now in the form of a spectrum, onto the focal plane. An array detector records the light preserving the horizontal distribution of light along the focal plane. In a spectrometer, a slit allows light over a selected narrow wavelength range to pass through to a detector.

2.6. LIBS advantages and disadvantages:

LIBS, like other methods of AES, are able to detect all elements and have the ability to provide simultaneous multi-element detection capability with lowabsolute detection limits. In addition, because the laser spark uses focused optical radiation to form the plasma, LIBS exhibits numerous appealing features that distinguish it from more conventional AES-based analytical techniques like inductively coupled plasma mass spectroscopy. These are: simple and rapid or real time analysis, the ablation and excitation processes are carried out in a single step; little-to-no sample preparation, which results in increased throughput and reduction of tedious and time-

consuming sample digestion and preparation procedures (this, however, can lead to a loss of accuracy through contamination). LIBS allow in situ analysis requiring only optical access to the sample. It can also be performed over a great distance, a technique referred to as *remote* sensing. Unlike remote analysis, in which some part of the LIBS system is close to the sample is the method of *stand-off* analysis. Here, the laser pulse is focused on to the sample at a distance using a long focal length optical system. Virtually any kind of sample can be analyzed: solids, liquids, aerosols, or gases. LIBS has the ability to analyze extremely hard materials which are difficult to digest such as ceramics, glasses and superconductors (Sirin Y, 2007).It is a non-destructive method, very small amount of sample (0.1 μg – 0.1 mg) is vaporized. It provides good sensitivity for some elements (e.g. Cl, F) difficult to monitor with conventional AES methods. In addition, LIBS has adaptability to a variety of different measurement scenarios, e.g. underwater analysis, direct and remote analysis, compact probe with the use of miniature solid state lasers, stand-off analysis. We can summarize LIBS advantages and disadvantages in the following table:

Table 2-1: Advantages and disadvantages of LIBS technique

Advantages	Disadvantages
1. Minimal (no) sample preparation.	1. Variation in the mass ablated caused by changes in the bulk matrix.
2.All states of matter can be analyzed, as well as conductive andnonconductivesamples.	2. Difficulty in obtaining matrix matching standards.

3.Very small amount of material is vaporized (around 10 of ng)	3. Detection limits higher (poorer) than standard solution technique (i.e. ICP-OES).
4.Easy analysis of refractory materials such as ceramics.	4. Poor precision, typically5 – 10 %.
5.Micro analysis is possible with spatial resolution of 1-10 μm.	5. Standard emission disadvantages, such as spectral interference self-absorption.
6. Capability of remote analysis in harsh environments.	6. Possibility of optical component damage from high energy density lasers.
7. Atomization and ionization are in one step.	7. Complexity
8. Capability of simultaneous multi-element analysis.	

2.7 LIBS applications:

LIBS is an emerging technique for elemental composition analysis. It can analyze and identify solid, liquid, and gas samples with little-to-low sample preparation. Figure (2-3) shows some examples(R. Payling,2000).

Figure (2-3) LIBS can analyze and identify samples in solid, liquid, and gas forms.

A benefit of LIBS technology is rapid, direct chemical characterization of solid samples without laborious dissolution procedures. LIBS has been used in a lot of areas. LIBS is well suited for the detection of nuclear and hazardous elements because it can be remote and standoff. For example, it has been used in the material composition analysis of nuclear power station steam generator tubes (L. J. Radziemski, Spectrochim. Acta, 2002), remote composition analysis of spent-fuel residuals, remote analysis of nuclear materials , in-situanalysis in the nuclear industry and detection of toxic and radioactive elements in sea water and ice (Zhang, S., et.al 2005).

The first reported industrial use of a fiber optic probe LIBS instrument was undertaken within the UK nuclear power generation industry in 1993. Because of the unique point sampling nature of the laser-induced plasma, LIBS can be applied for analysis of aerosols (Milonni, P.W. andEberly, J.H., 2010).

An aerosol is a suspension of fine solid particles or liquid droplets with characteristic dimensions in the nanometer to micrometer range in a gas. The

analysis of aerosols is very important for industrial hygiene and clean room technology. Conventional laboratory-based techniques such as atomic absorption spectroscopy (AAS), inductively coupled plasma optical emission spectroscopy (ICP-OES), and inductively coupled plasma mass spectroscopy (ICP-MS) can determine the chemical composition of aerosols after filter collections. However, these techniques usually require time-consuming and labor-intensive and expensive procedures. LIBS can directly analyze aerosols in an on-line and in-situ fashion. Furthermore, LIBS can also perform quasi-continuous analysis of automatically sampled filters or on a filter band. Process control is expected to be a significant LIBS application in the future. Due to the poor accuracy and precision of LIBS, there is certainly room for future improvement in the aerosol LIBS. LIBS has many applications in industry. In the metals and alloys processing industry, there are increasing requirements for quality and productivity control of on-line chemical compositional analysis. Since LIBS can directly sample the specimen in the product line by the laser itself, LIBS is predestined for this task. For example, automatic inspection equipment called LIFT (laser identification of fittings and tubes) based on LIBS has been developed to prevent any mix of material grades, which can inspect more than different material grades (Milonni, P.W., andEberly, J.H., 2010). In steel industry, LIBS is applied to quantitative slag analysis and liquid steel analysis. It is believed that there will be more and more industrial applications of LIBS in the future. The analysis of biological and medical samples is another interesting LIBS application. The knowledge of the presence or absence of certain elements in the human body is of vital importance. For example, the accumulation of cadmium (Cd) or mercury (Hg) in excess concentration may have toxic effects. LIBS provide a

simpleand fast qualitative and quantitative elemental analysis of solids. Researchers have done extensive work in the analysis of calcified tissue materials, teeth, bones, human hair, plants, and some other biological samples. Because of the poor statistics, reproducibility, and sensitivity of LIBS, these kinds of applications are still in their infancy. LIBS can be used for surface and three-dimensional mapping of target elements. For example, LIBS is expected to be a quick method to measure the surface and internal distribution of many pharmaceutical materials in the pharmaceutical industry. Figure (2-4) shows a LIBS system for the pharmaceutical industry which is commercialized by Pharma Laser. Microanalysis of tool steel and microelectronics with LIBS has been studied recently.

Figure (2-4) LIBS instrument for pharmaceutical industry.

2.5 Literature review:

In 2009, Y. Godal, M.T. Taschuk, S.L. Lui, Y.Y. Tsui and R. Fedosejevshave demonstrated that by the resonant dual-pulse technique the sensitivity of the LIBS can be increased with orders in magnitude reduction in the ablation pulse energy, which makes the realization of a field portable spectrometer more realistic. Even though in the 100 ppb range for Pb significant improvements can be made. Possible approaches are to increase the resonant pulse energy,

improve the collection optics and integrate more shots using higher repetition rate lasers. In addition, a more sophisticated analysis of the rejection and an emission line fitting approach may be employed. A 2D map of a fingerprint on a Si wafer has been successfully acquired using 5 μJ pulses, demonstrating that fiber or microchip lasers with kHz repetition rates could be used as the excitation source for a portable μLIBS fingerprint scanner. These μLIBS techniques can also be applied to microfluidic Lab on Chip applications for the measurement of elemental content of micro specimens of fluids. Considerable work is still required in order to determine the optimum configuration and limit of detection obtainable for such systems.

In 2011, X. Fang and S.R. Ahmad proved that laser-induced breakdown spectroscopy allows detection of mercury in aqueous matrix at a ppb level of concentration using pre-concentration of target species. Pre-concentration has been most effectively carried out on a metal plate by electrolysis before subjecting the plate to LIBS analysis. A pre-concentration factor of ~180 for the mercury determination in triple-distilled water was achieved. This has greatly increased the capability and applicability of LIBS for trace metal detection in water. Such improvement has been achieved from its previous status where mercury detection in water at concentrations of even a few thousands ppm was difficult by direct LIBS probe in water bulk medium and for solid sample the reported limit of detection for mercury was just above ppm level. Their study is an initial evaluation of the pre-concentration method as assistance for LIBS. The further investigation is being undertaken to optimize the technique to even further lower limit of detection and improve the sensitivity and reproducibility of LIBS for the detection of heavy metals including mercury in water. Possible industrial applications of

LIBS for aqueous samples with such pre-concentration method are also being explored.

In 2012 Qassem I, et. al.reported that a LIBS-based bacterial identification could be successfully applied to identify pathogens in a clinical specimen. The issue of mixed samples has once again been addressed with mixtures prepared from two closely related bacteria (E. coli and E. cloacae) using clinically relevant and realistic mixing fractions. Their work was intended to represent situations of clinical infections with the presence of additional background or contaminant bacteria. To simulate the use of a LIBS-based test to diagnose urinary tract infections, cells of S. epidermises were spiked into sterile urine samples and the bacteria were harvested from these samples with no other preparation or washing. Using a discriminant function analysis model that contained spectra from S. epidermises cells harvested from water as well as two other staphylococci species, the urine-harvested samples were identified with 100% accuracy. No spectrum, used to construct the model, was obtained from cells obtained from a urine sample. A 669-spectrum library composed of spectra from five bacterial genera and 13 distinct taxonomic groups was compiled and tested using external validation techniques where the model did not contain any spectra from samples acquired at the same time.Little difference was observed between the five-class model and the 13-class model. Truth tables constructed from the external validation of the five genus model yielded sensitivities of approximately 85% and specificities above 95%. These external validation testswere compared to LOO cross-validation tests and, as expected, an artificially high accuracy was observed in the LOO tests. Last, the use of sequential classification testing was investigated by identifying closely related E. coli and E. cloacae spectra using first the five-

genus model spectral library and then a more targeted model that contained only E. coli and E. cloacae spectra. The improvement in accuracy obtained by using the more targeted model demonstrated the utility of using sequential testing to “filter” unknown spectra as they are tested, first through a “coarse” (perhaps genus-level) model and then through a more “fine” species-level (or similar) model to eventually obtain an accurate identification at the desired level. This simple addition of sequential testing can be easily implemented with little to no increase in complexity or time required.

In 2013 Tomoko Takahashi, et. al. used Long-Pulse Laser-Induced Breakdown Spectroscopy for analysis of the composition of rock and sediment samples submerged in seawater to investigate the application of Laser-Induced Breakdown Spectroscopy to qualitatively analyze the composition of various seafloor rock samples in seawater. They achieved well-resolved emission spectra of submerged samples by using a long laser pulse of duration 250 ns. They found that the main elements in each rock sample could be successfully identified both in pure water and in seawater. When comparing the measurements made in pure water and in seawater, some effects of the seawater could be seen. The results suggested that long-pulse LIBS may be applicable for in situ, multi-element chemical analysis of sediments and rocks in the marine environment.

1n 2014, PeichaoZheng, et. al. determined trace mercury in an aqueous solution using laser-induced breakdown spectroscopy with the assistance of a solution cathode glow discharge (SCGD) system. They converted the aqueous solution to the gas phase using a high voltage DC discharge, and then the generated mercury vapor was cooled by a gas–liquid separator to improve the concentration of the mercury. Finally, a 1064 nm wavelength

Nd:YAG laser was used to produce the plasma. Characteristic spectral line of HgI 253.65 nm was selected for the analysis, under the optimal conditions of LIBS, to investigate the influences of the acid anion, the discharge current, the sample flow rate and the carrier gas flow rate. The temporal behavior of the electron temperature and electron number density were also investigated; From the results, they showed that the electron temperature decreases from about 10900 K to 8800 K with a delay time from 200 ns to 6 μs and that the electron number density is in the orders of 10^{17} and 10^{18} cm^{-3}, and decreases with delay time. They evaluated the analytical performance of this method under optimized conditions, and a calibration curve of Hg was plotted based on the different concentrations measurement results, and the detection limit (LOD) of Hg was calculated to be 0.36 mg L^{-1}. By this experimental configuration, the detection limit and sensitivity of Hg are improved to some extent.

In 2014 Qi Shi, et.al. Combined nano-channel material with laser induced breakdown spectroscopy (LIBS) to achieve sensitive and quick detection of metal ions in liquid samples. A 3D anodic aluminum oxide porous membrane (AAOPM) was selected as a novel substrate for the first time, which showed excellent potential for liquid analysis. It is worth mentioning that the LIBS signal of the target elements in aqueous solution dropped on the 3D AAOPM was increased by up to 19 times in comparison with that on the tablet sample made of aluminium oxide powder. The attractive results were mainly attributed to the peculiar structure of the 3D AAOPM. Firstly, an abundant strong coordination metal–oxygen bond between hydroxyl groups and metal ions existed on the surface of the novel substrate. Secondly, the extremely high aspect ratio of the 3D AAOPM could supply a much larger contact area between the matrix and analytes. Thirdly, the

special nano-channel distribution could make efficient coupling of a laser beam with the materials. Finally, the sample pervasion and volatilization could be finished within a very short time because of the micrometer level thickness and porosity of the 3D AAOPM. The calibration curves with linearity ranges (1–100 μg mL^{-1}) and good linearity (R squared better than 0.983 for all of the four target elements) were established, and the limits of detection (LODs) obtained were 0.18 μg mL^{-1}, 0.12 μg mL^{-1}, 0.081 μg mL^{-1}, and 0.11 μg mL^{-1} for Cu^{+2}, Ag^{+1}, Pb^{+2}, and Cr^{+3}, respectively. In real sample analyses, the recoveries of three elements at different concentration levels were all in the range of 92.5–107.4%, with the relative standard deviations of parallel samples around 10.0%. This novel method showed a fast, simple and super sensitive monitoring tool for liquid sample analysis compared with the traditional LIBS method.

In 2015 Nafie A. Almuslet and Maria M. Osman usedLaser Induced Breakdown to Investigate the Metals in DairyProducts Waste Water. The analysis of the industrial water samples using LIBS technique led to the determination of different heavy metals.The concentrations of heavy metals (Cr, Co, Fe, Mg, Ti, Mn, and Hg, present in waste water samples, were estimated. Cr and Hg atoms were appeared in all samples with different concentrations at different pulse energies, these atoms are highly toxic. This study reveals that the waste water samples collected from diary plant are contaminated by several toxic elements Titanium, chromium, and Mercury. Most of these elements are considered as highly toxic and carcinogens. They could cause a lot of problems for heart and lungs deceases.

CHAPTER THREE

MATERIALS AND METHODS

3.1 Introduction:

This chapter describes the way of experimental work, and the setup parts. The equipments used in measuring and recording data of materials are mentioned. The methodof investigation of different water samples that collected from different places in Khartoum State in Sudan is described. LIBS technology provides a rapid elemental analysis of solids, liquids, and gases with little or no sample preparation .In LIBS technique, a strong laser pulse evaporates a small amount of material under the test by creating a plasma plume. The Nd:YAG laser used in this work candeliver maximum pulse energy of 1 J with a pulse width of10 ns and operate at a 2 Hz pulse repetition rate, operating inQ-switched mode. Here, 1064 nm radiation emitted at afundamental frequency from Nd: YAG laser was appliedfor the production of the plasma spark at the testedsamples.

3.2 The samples:

The materials used were eight water samples collected from different locations in Khartoum State in Sudan: (Khartoum, Bahri and Omdurman).

3.3 The collection of the samples:

The samples were collected from sources of water in Khartoum State in Sudan in plastic bottles. All bottles were thoroughly washed with Distilled water. Eight water samples were collected and investigated in this work.

3.4 The experimental setup:

The experimental setup used in this work was arranged as shown in figures (3-1) and (3-2)

Figure (3-1): The experimental setup.

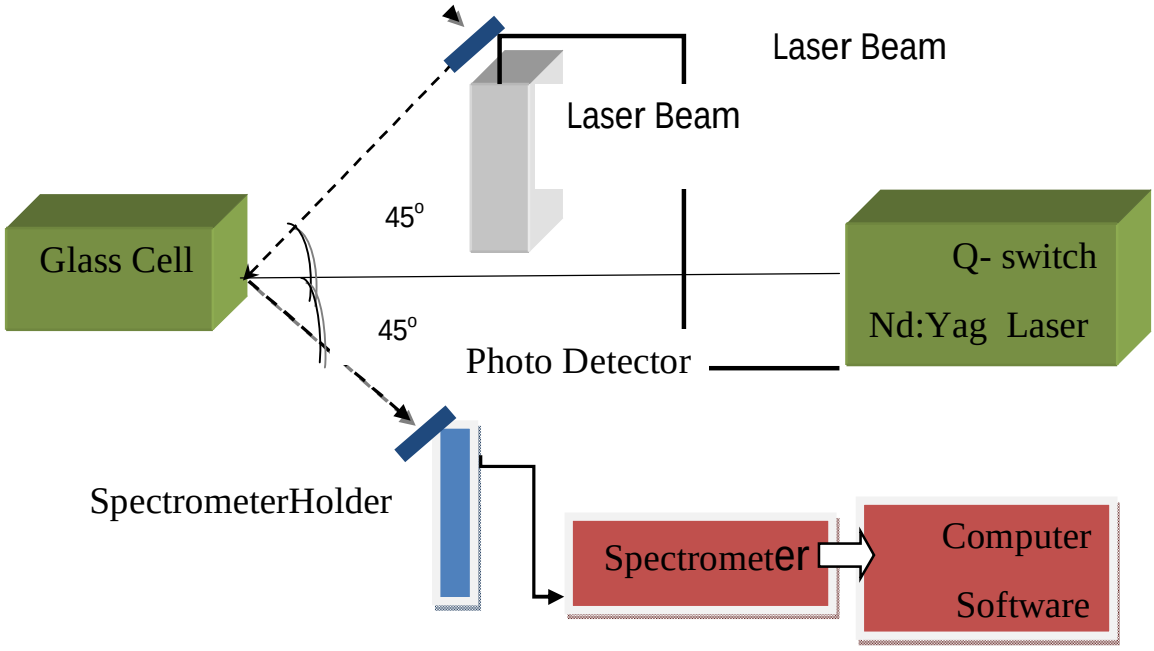

Figure (3-2): Schematic diagram of the setup.

The setup was consisted of:

3.4.1 The laser:

Q swichedNd – YAG Laser System structure is mainly consisted of the following units:Power Supply, Laser handpiece, control unit and cooling system.The power supply is assembled in the main case. The specifications of the Nd – YAG laser used in this work are listed in table (3-1).

Table (3-1) laser specifications

component	**Specifications**
Company	Shanghai Apolo Medical Technology Co., Ltd China
Power supply:	~230V, 50/60Hz
Model	HS-220
Laser type	Q switched Nd – YAG Laser
Laser wavelength：	1064nm & 532nm
Weight	20 kg
Pulse width：	10ns
Repeat frequency	1,2,3,4, 5HZ
Lead light method	directly export laser
The light spot diameter	2~8mm
Power supply	90-130V, 50Hz/60Hz or 200-260v, 50Hz
Environment temperature：	5˚C～40˚C
Relative humidity：	≦80%
Cooling system	The water-cooling + the air cooling inside. System device overview

Figure (3-3): Front view of the Nd-YAG laser.

1 .Laser hand piece

2. Emergency switch

3. Main host

4. Key switch

5. LCD control panel

6. Hand piece Connector.

(i) Emergency switch:

While appearing the urgent circumstance, pressing it, the power will be cut off. Revolving the switch according to arrowhead direction, the power supply renews.

(ii) Key switch:

Whole switch of power.

(iii) SIMMER key：

At the “Operation Interface-SIMM”, this key can make the instrument enter the situation from S (Standby) to R (Ready) mode.The xenon flash lamp is triggered for and may go further to work mode. Pressing “SIMMER” key

again, the system will escape from ready to standby and the xenon flash lamp is off.

(v) MENU key:

At the “Operation interface-FREQ”, this key can set the frequency of each second from 1 to 5 Hz.

(iv) Up key:

At the “Operation interface-PWR+”, this key system enters the interface of power energy adjustment; Press again, can increase the power energy

(vi) Down key:

At the “Operation interface-PWR-“, this key, system enters interface of power energy adjustment; Press again, can decrease the power energy.

(vii) Enter key:

This key, can make the machine select Laser wavelength 1064nm or 532nm when it is on the standby mode. Or when the system is ready on “Operation interface-R”, pressing this key enters the system to “W” work mode. The work appearance, press the foot switch, the Laser output for treatment. Or when the system is in working mode on “Operation interface-W”, press this key the system will escape from work to ready mode. Press Simmer key again; the system will enter to standby mode.

(viii) The temperature display and protection:

The system has the temperature display function, which can monitor the temperature of the circulating water, when the temperature of the circulation water exceed prescriptive protection Temperature,” the water temperature lead high" will show on the screen, at the same time the Buzzer gives an alarm and the instrument won't continue to work. When the temperature of circular water declines under the protect temperaturethe instrument can work normally.

(vv) The water current display and protection:

The system has the water current display function, which can monitor the current of the circulating water.When the current of the circulation water declines under prescriptive Protection current," the water current lead low" will show on the screen, at the same time the Buzzers give an alarm and the instrument won't continue to work. When the water current of Circular water exceed the protect currentthe instrument can work normally.

3.4.2The glass cell:

Aglass cell was used to put the samples inside it, the dimensions were 5.64cm x 3.84cm x 2.42cm**.**

3.4.3 The Optical System:

This system consisted of mirrors and concave lenses.

3.4.4 The Detection System:

The detection system was consist of:

1- The spectrometer: The spectrometer used in this work was Ocean Optics LIBS 4000+ Its model USB4-UV/VIS, with dimensions (in mm): 89.1 x 63.3 x 34.4, Fig (3-4) shows the internal components of this spectrometer.

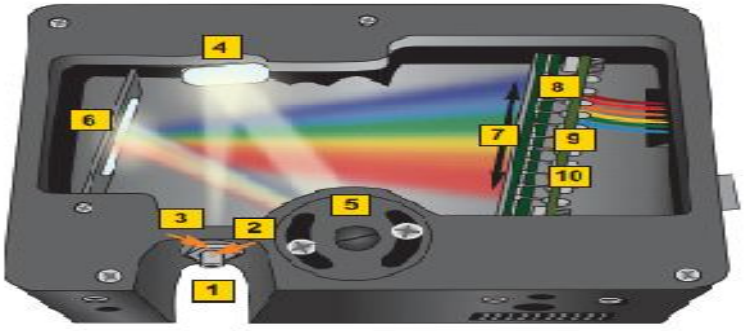

Figure (3-4): The USB4000 Spectrometer.

The USB4000 interfaces to computer with Windows operating system. The modular USB4000 is responsive from 200-850 nm and it can be configured with various Ocean Optics optical bench accessories, light sources and sampling optics to create application-specific systems for thousands of absorbance, reflection and emission applications.

The USB4000 has signal to noise of 300:1 and optical resolution (FWHM) ranging from 0.03-8.4 nm (depending on the grating and entrance aperture selection). The detector was Toshiba TCD1304AP linear CCD array detector range: (200-850) nm, with 3648 pixels of size (8 μm x 200 μm) and Pixel well depth about 100,000 electrons with sensitivity: 130 photons/count at 400 nm; 60 photons/count at 600 nm. The grating of the spectrometer type is 600 lines blazed at 300 nm.

The USB4000 interfaces to a computer via USB 2.0. Data unique to each spectrometer and is programmed into a memory chip on the USB4000; spectra suite spectroscopy operating software reads these values for easy setup and hot swapping among computers, whether they run on Linux, Mac or Windows operating systems. When connected to a computer via USB, the USB4000 draws its power from the computer.

1- **SMA 905 Connector**:

Light from a fiber enters the optical bench through the SMA 905 Connector. The SMA 905 bulkhead provides a precise locus for the end of the optical fiber, fixed slit, absorbance filter and fiber clad mode aperture.

2- **Fixed Entrance Slit**:

Light passes through the installed slit, which acts as the entrance aperture. The slit is fixed in the SMA 905 bulkhead to sit against the end of a fiber.

3- **Long pass Absorbing Filter:**

An absorbance filter is installed between the slit and the clad mode aperture in the SMA 905 bulkhead. The filter is used to block second- and third order effects or to balance color.

4- **Collimating Mirror:**

It is matched to the 0.22 numerical aperture of the optical fiber. Light reflects from this mirror, as a collimated beam, toward the grating. One can install a standard mirror or a UV absorbing SAG+ mirror.

5- **Grating & Wavelength Range:**

Installed on a platform that rotate to select the starting wavelength that have specified. Then the grating permanently fixed in place to eliminate mechanical shifts or drift.

6- **Focusing Mirror:**

This mirror focuses first-order spectra on the detector plane. Both the collimating and focusing mirrors are made in-house to guarantee the highest reflectance and the lowest stray light possible.

7- **L4 Detector Collection Lens:**

This cylindrical lens, made in-house to ensure aberration-free performance, is fixed to the detector to focus the light from the tall slit onto the shorter detector elements. It increases light-collection efficiency.

8- **Detector:**

There is 3648-element Toshiba TCD1304AP linear CCD array detector. Each pixel responds to the wavelength of light that strikes it. Electronics bring the complete spectrum to the software.

9- **OFLV Variable Long pass Order-sorting Filter:**

The proprietary filters precisely block second- and third-order light from reaching specific detector elements

10- **UV4 Detector Upgrade:**

The detector’s standard BK7 window is replaced with a quartz window to enhance the performance of the spectrometer for applications <340 nm.

3.4.6 The software system:

The software "Spectra Suite" usedin this work is shown in figure (3-5). This software can easily manage multiple USBspectrometers – each with different acquisition parameters inmultiple windows, and provides graphicaland numeric representation of spectra from each spectrometer.

Spectra Suite allows to perform the three basic spectroscopic experiments absorbance, reflectance and emission – as well as signal-processing functions such as electrical dark-signal correction, stray light correction, boxcar pixel smoothing and signal averaging. Using Spectra Suite, one can combine data from multiple sources for applications that include upwelling /down welling measurements, dual-beam referencing and process monitoring.

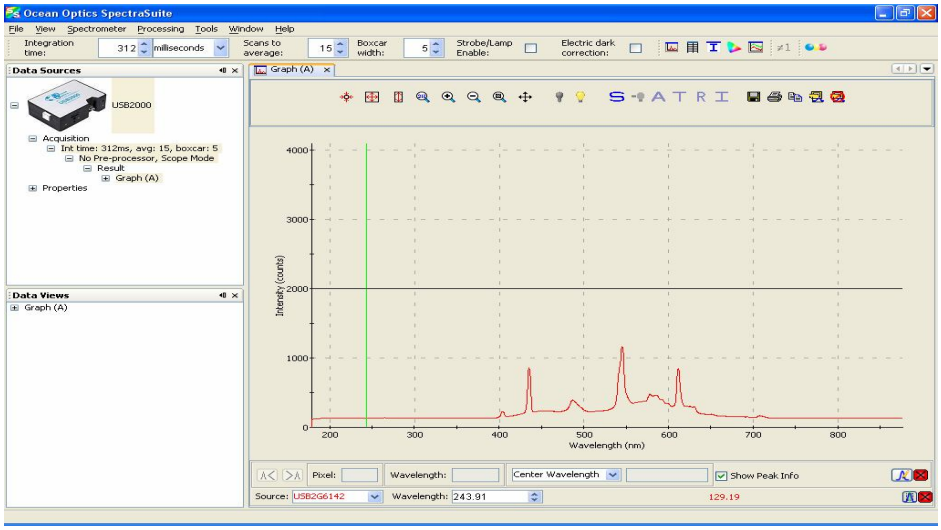

Figure (3-5) the spectrum of the emitted intensity of the sample.

(i) The computer system:

The optical fiber was connected to the computer system to show the emitted intensities' of the sample.

3.5 Electricity and instrument safety:

When the laser instrument is used by 220V or 110V, the power supply capacity is not less than the 1000 W.The net power source that connects with laser instrument must match international single-phase three line Alternative Current (AC) outlets with good connection with the ground; the specification is above10A, connecting the ground well is very important. When the laser treatment stops, the high-pressured component still remain high voltage. Opening the protection cover of machine may be shocked by high pressure. Insuring the stability of the electric voltage. Sealing up all panels and the behind cover. Opening the behind cover may produce danger as well.

3.6 Methodology:

The experimental procedure was done as follows:

- The setup was arranged as shown in figure (3.1)
- The laser energy was adjusted by adjusting the flash lamp voltage in order to obtain sufficient peak power need to form plasma.
- Then the spectrometer was connected to the PC through USB cable and the program spectra suit was launched.
- A laser pulse was focused on the surface of the sample cell without the sample and the spectrum was recorded and saved as dark spectrum that would be subtracted when getting the sample spectrum.
- The eight samples wereirradiated by the laser with different pulse energies (60, 80,100 and 120 mJ).

- The sample emission spectrum was processed by subtracting the dark spectrum.
- The result was captured by the spectrometer, and the relation between wavelength and intensity was plotted using origin program. The emitted spectra were analyzed using Atomic spectral database.
- By referring to the atomic spectra database, theelementsineach sample were identified from the graphs.
- The same above procedures were done for all samples.
- A comparison was done between the components of the samples and their intensities.

Chapter Four

Results and Discussion

4.1 Introduction:

This chapter presents the data collected from the experimental work, in figures, and tables. The data was analyzed and discussed. The LIBS emission spectra were recorded at an angle of 90˚ to the direction of incident laser pulse. Software built in the spectrometer reads the data from the chip and reconstructs the spectrum. This makes it possible to measure a wide wavelength range simultaneously with high spectral resolution (0.03 nm).

The primary advantage of LIBS for liquid samples, such as the samples in this study, is that it can be used toidentify and analysis elements without any pretreatment and sample preparation. In this study quantitative and qualitative results were obtained for eight water samples after irradiation with different laser energies.

4.2 The results:

4.2.1 Irradiation with 60 mJ:

Figures (4-1) to (4-8) show the LIBS emission spectra for the eight water samples, respectively, after irradiation with 60 mJ pulse energy.The spectra were recorded in the region from 200 nm to 850 nm.

Atomic spectra database, and Hand book of Basic Atomic Spectroscopic Data were used for the spectral analysis of the samples.Table (4-1) lists the analyzed data for the eight samples,where the wavelength of each emitted line (λ) was characterized by its intensity (I).

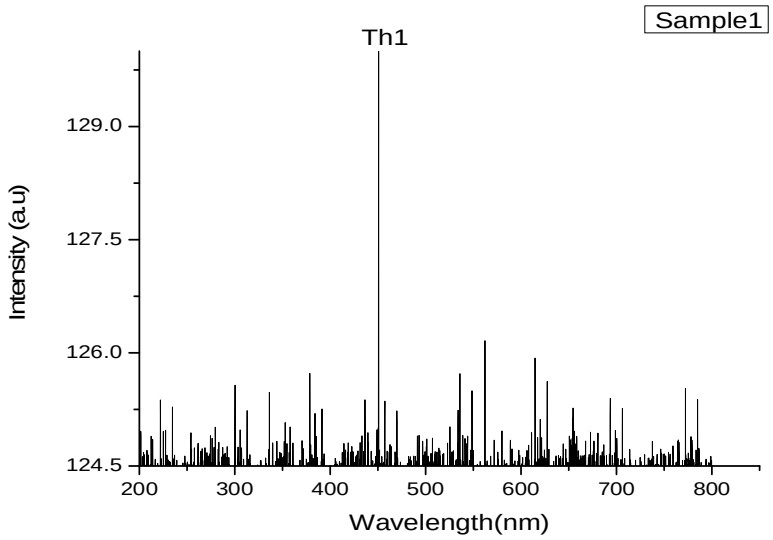

Fig (4-1) LIBS emission spectrum of sample1 after irradiation by 60 mJ.

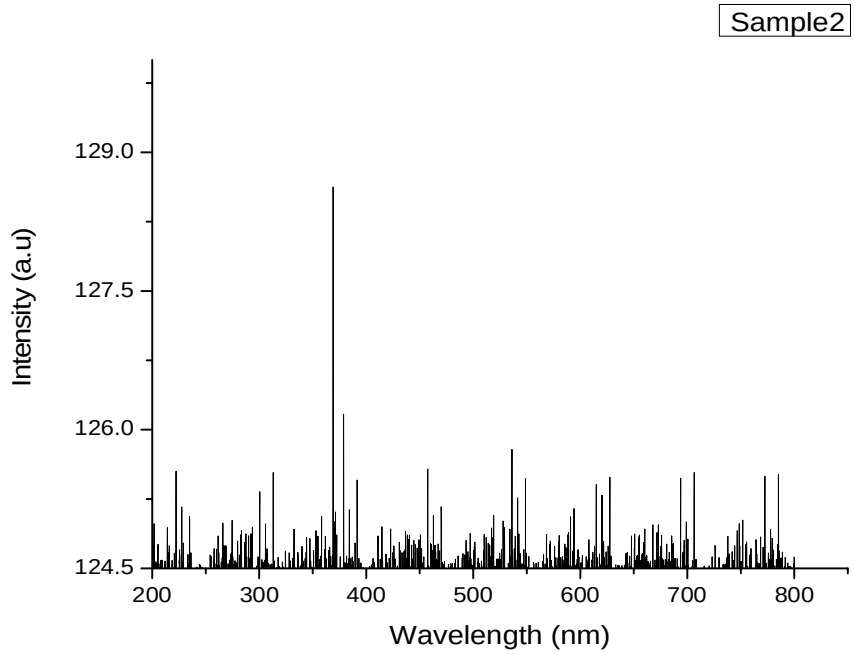

Fig (4-2) LIBS emission spectrum of sample2 after irradiation by 60 mJ.

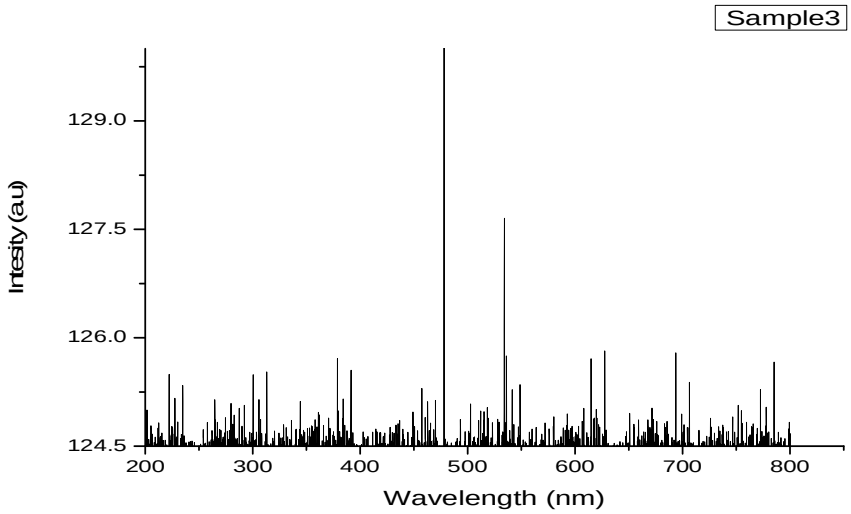

Fig (4-3)LIBS emission spectrum of sample3 after irradiation by 60 mJ.

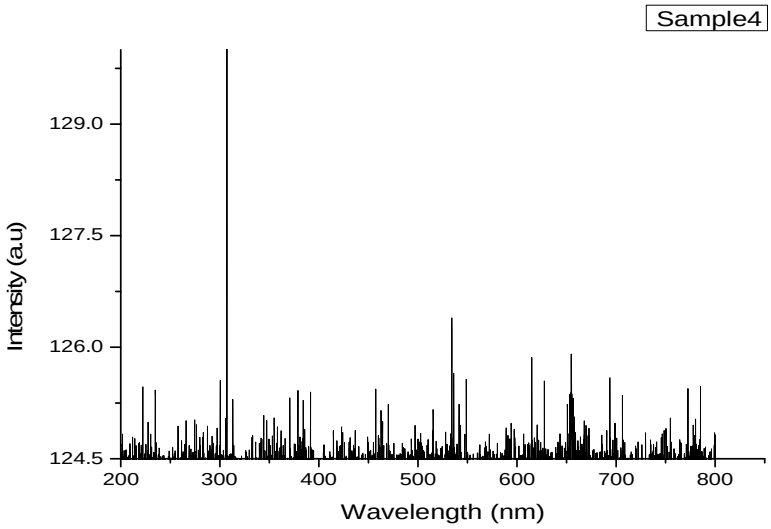

Fig (4-4) LIBS emission spectrum of sample4 after irradiation by 60mJ.

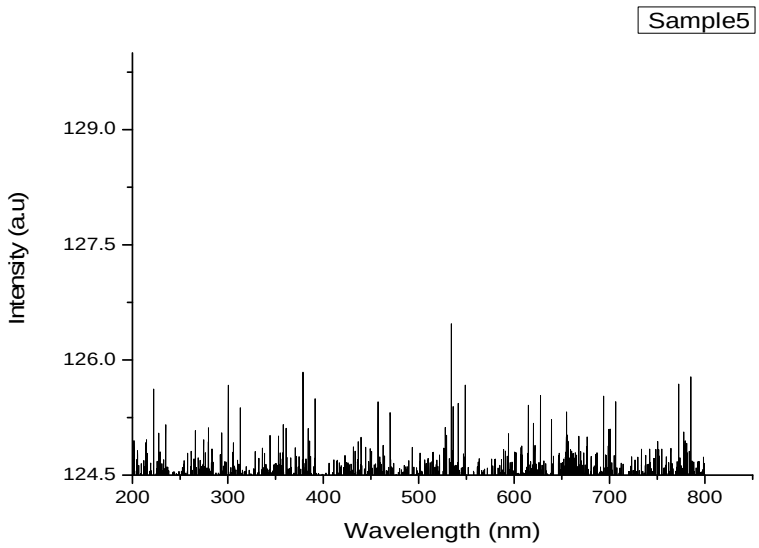

Fig (4-5) LIBS emission spectrum of sample5 after irradiation by 60

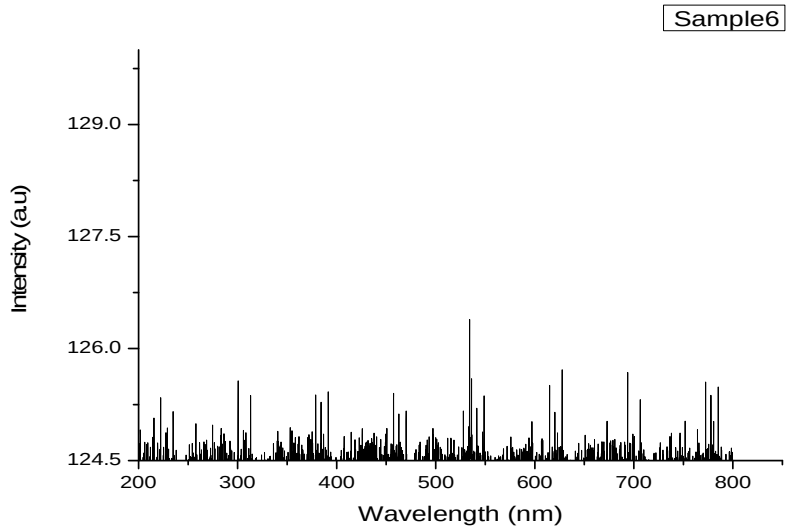

Fig (4-6)LIBS emission spectrum of sample6 after irradiation by 60 mJ.

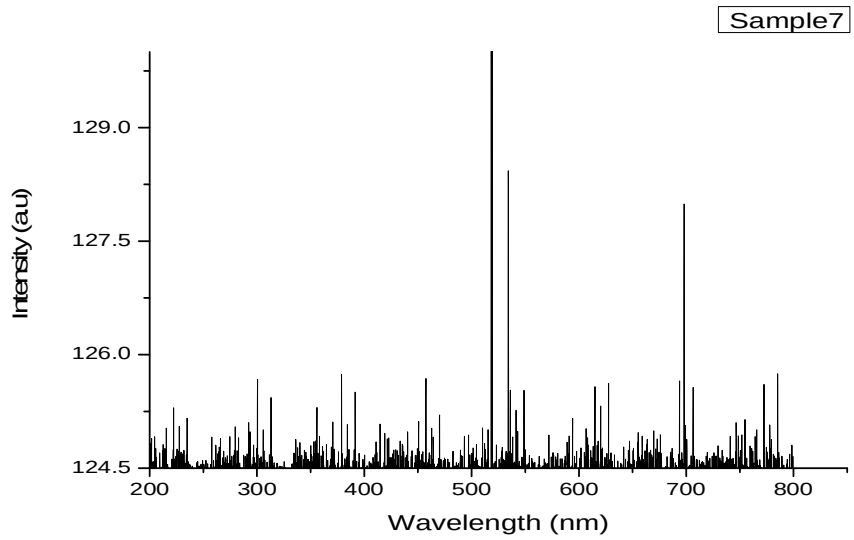

Fig(4-7) LIBS emission spectrum of sample7 after irradiation by 60 mJ.

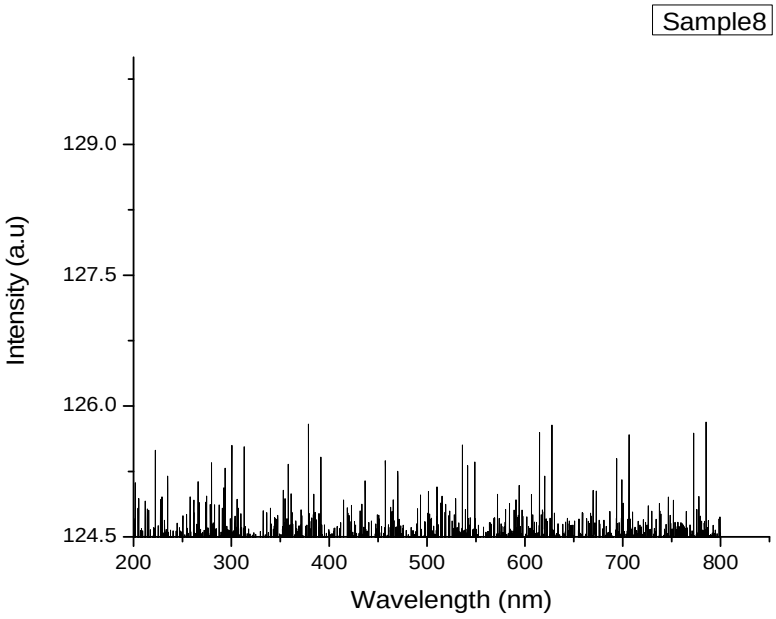

Fig(4-8) LIBS emission spectrum of sample8 after irradiation by 60 mJ.

Table (4-1): The analyzed data of the eight samples irradiated by 60mJ:

Element	λ (nm)	I_{S1} (a.u)	I_{S2} (a.u)	I_{S3} (a.u)	I_{S4} (a.u)	I_{S5} (a.u)	I_{S6} (a.u)	I_{S7} (a.u)	I_{S8} (a.u)
Ni I	222.29 336.57	125.63 125.51	125.81	125.76	125378	125.68	125.66	125.66	125.88
Ni II	227.8	125.14	124.99	125.02	125.50	125.91	125.68	125.02	125.50
As I	234.98	125.56	125.36	125.58	125.73	125.14	125.46	125.48	125.51
As II	225.31	125.10	125.00	-------	125.01	125.43	125.46	-------	125.01
Ru I	300.55	125.89	125.61	125.81	125.81	125.10	125.00	126.01	125.86
Th I	378.91 436.59 451.05	125.71 125.68 130.26	128.90 126.44	125.98	125.76	125.98	125.81	126.06	126.61
Th II	299.06 635.90	124.14 125.25	124.00	123.92 124.00	124.35	126.14	126.01	--------	124.35
Th III	358.28	125.15	125.01	125.12	------	------	------	123.92	------
Zr I	457.55	125.66	125.83	125.33	125.76	124.14	124.00	124.00	-------
Zr II	738.28	124.95	124.59	124.78	124.99	125.25	125.01	125.12	125.50
Tb I	470.24	125.53	125.43	126.01	125.48	125.15	125.70	-------	124.99
Eu I	537.69	126.26	126.06	------	------	-------	125.73	125.98	125.53
Li I	548.51	125.38	125.78	125.51	125.86	125.73	124.59	124.78	125.83
I I	562.56	125.94	---------	------	------	124.95	125.51	125.48	125.68
Cu I	615.03	125.16	125.73	126.01	126.21	125.63	126.06	------	126.01
Xe I	627.75	125.26	125.78	126.11	125.83	126.26	125.58	125.83	125.76
K I	693.87 534.29	125.68	125.76	126.01	126.74	125.96	126.05	125.95	-------
He I	706.57	125.53	125.81	125.61	125.66	125.81	126.01	126.01	125.98
Ne I	772.46	125.84	125.78	125.53	125.73	125.81	126.71	-------	125.73
Cs I	782.25	125.71	125.83	125.94	125.78	126.79	125.66	125.88	126.14
Cs II	358.28	125.30	125.00	125.30	125.49	125.73	125.78	125.53	125.49
Cs III	353.30	125.22	125.12	125.30	125.41	125.98	125.83	126.09	125.41
Hg I	313.18	--------	125.86	125.76	125.61	126.06	125.83	125.30	125.81
Cr I	391.62	--------	125.76	125.81	125.66	125.30	125.12	125.30	125.73
Cr II	353.20	126.20	126.21	126.35	126.58	125.22	125.70	125.76	126.58
Cr III	204.84	124.83	124.56	124.66	124.34	125.68	125.71	125.81	124.34
Cu I	615.03	--------	-------	126.11	126.21	125.83	126.21	126.35	126.15
Na I	654.77	--------	-------	--------	126.01	126.20	124.56	124.66	126.10
Fe I	370.79	--------	-------	-------	125.68	124.83	125.86	125.91	-------
Fe II	369.84	124.98	124.50	--------	125.00	125.66	125.80	126.00	125.61
Fe III	208.59 227.81 492.65	124.88 124.98 125.07	125.00	124.98 125.02	125.02	-------	-------	--------	125.68
Tl I	307.29	--------	---------	--------	130.33	--------	-------	128.75	---------
Tl II	213.75	125.06	125.10	125.15	125.24	--------	-------	128.53	125.88
Tl III	391.56	125.40	125.53	125.59	125.63	--------	---------	130.33	125.50

4.2.2 Irradiation by 80 mJ:

The spectra of the eight samples were recorded in the same region after irradiation by 80 mJ laser pulse, as shown in figures (4-9) to (4-16).The recorded spectra were analyzed and the identification of each spectral lineis listed in table (4-2).

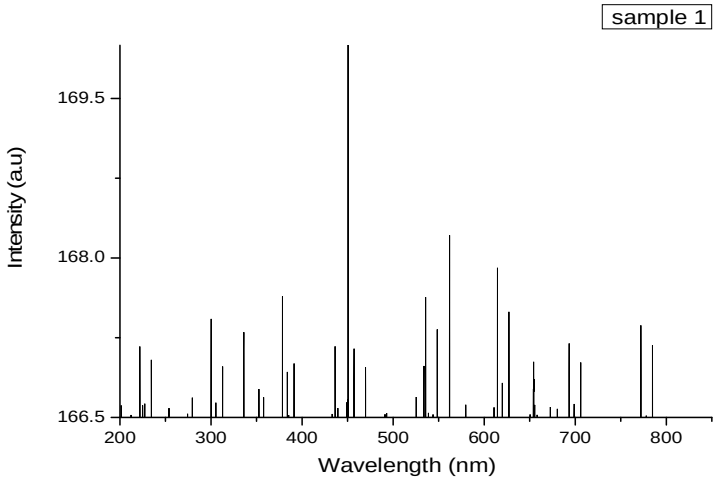

Fig (4-9) LIBS emission spectrum of sample1 after irradiation by 80 mJ.

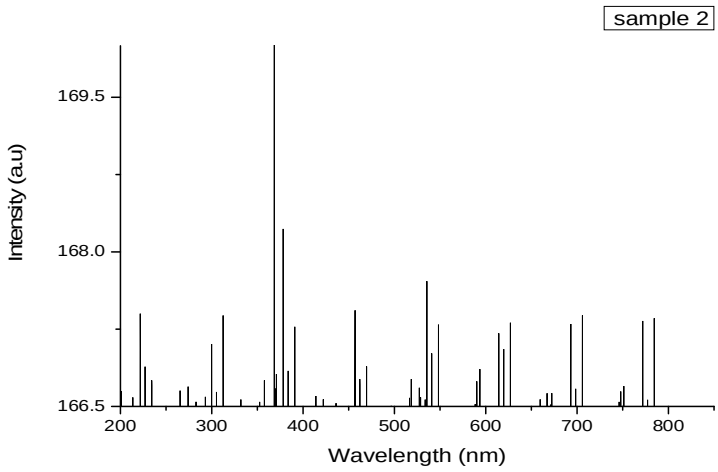

Fig(4-10) LIBS emission spectrum of sample2 after irradiation by 80 mJ.

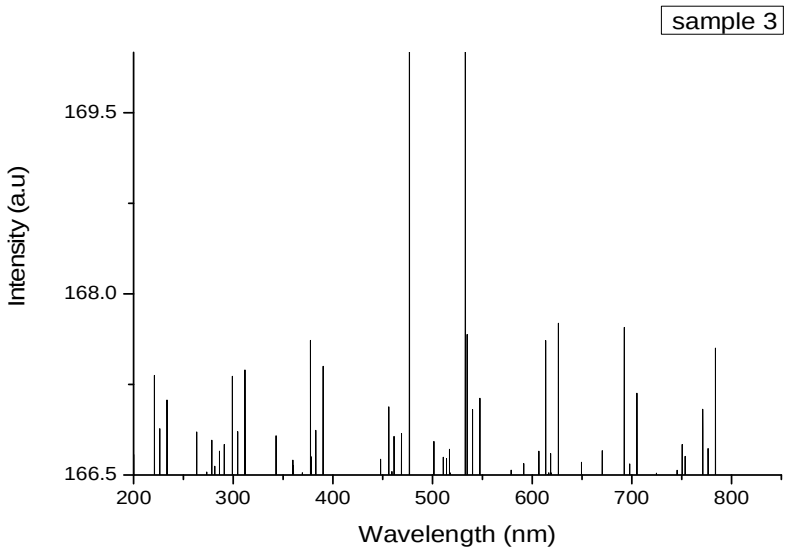

Fig(4-11) LIBS emission spectrum of sample3 after irradiation by 80 mJ.

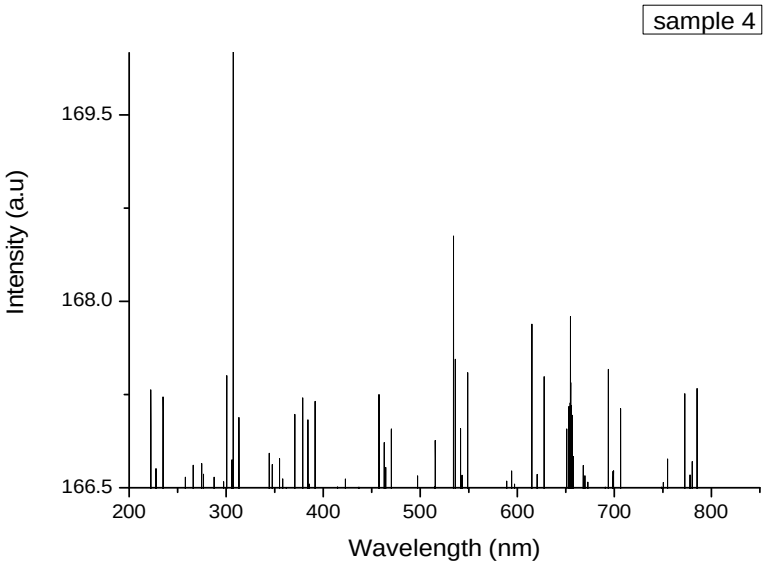

Fig(4-12) LIBS emission spectrum of sample4 after irradiation by 80 mJ.

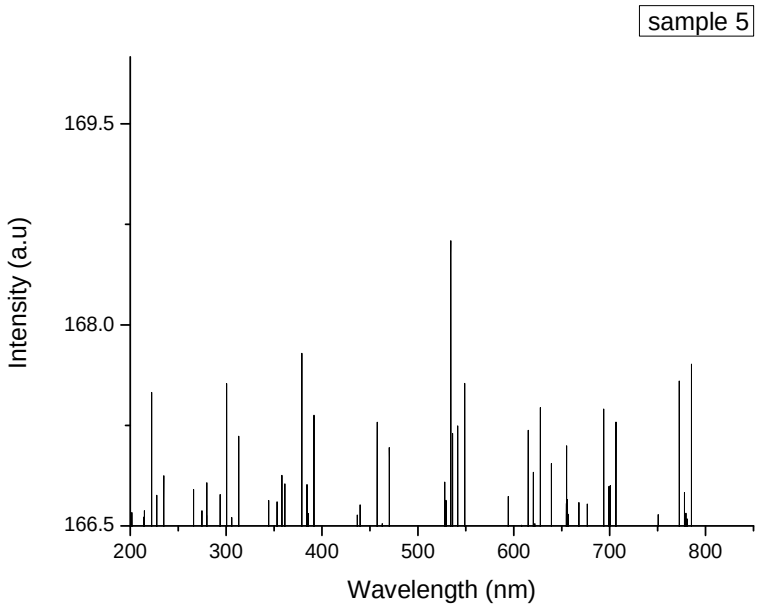

Fig(4-13) LIBS emission spectrum of sample5 after irradiation by 80 mJ.

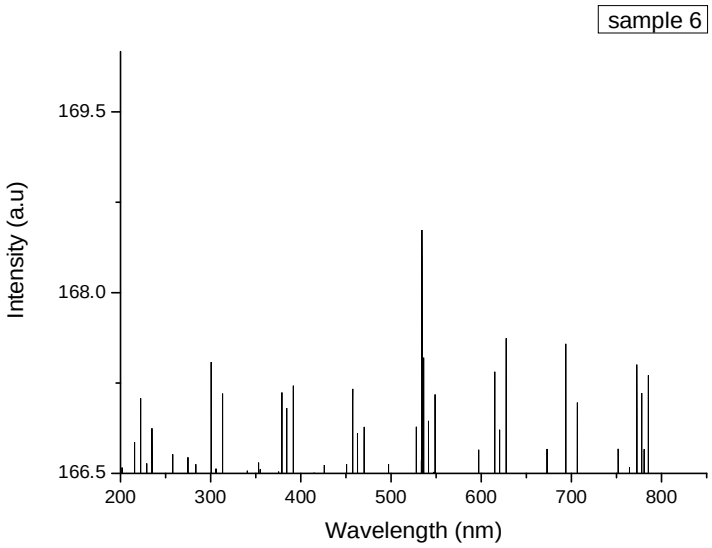

Fig(4-14) LIBS emission spectrum of sample6 after irradiation by 80 mJ.

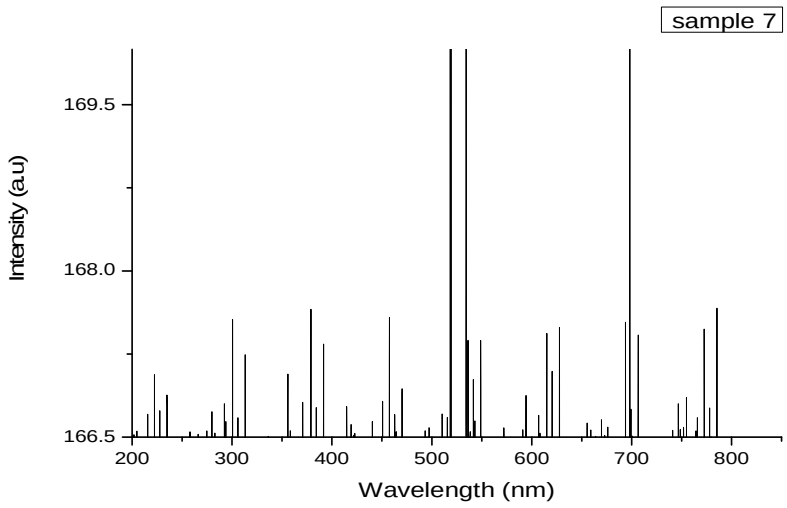

Fig(4-15) LIBS emission spectrum of sample7 after irradiation by 80 mJ.

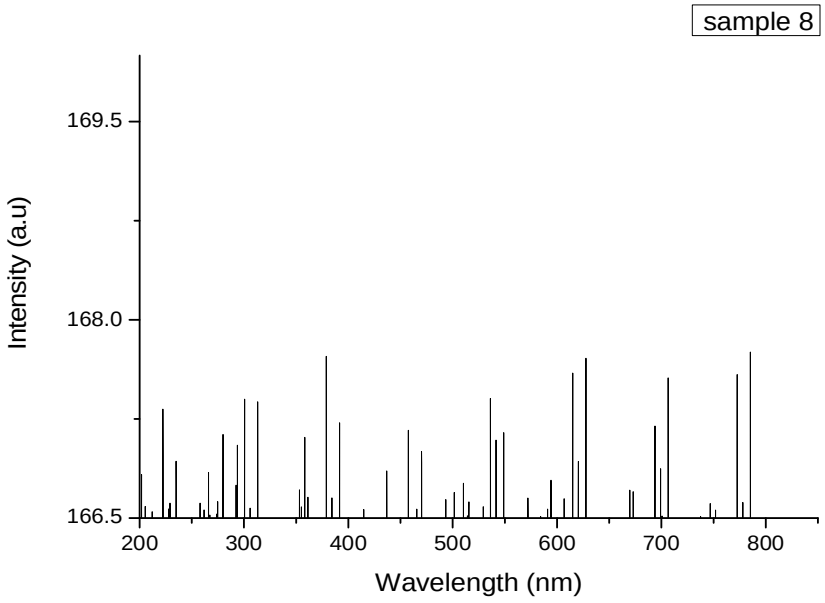

Fig(4-16) LIBS emission spectrum of sample8 after irradiation by 80 mJ.

Table (4-2) the analyzed data of the eight samples, after irradiation by 80 mJ:

Element	λ (nm)	I_{S1} (a.u)	I_{S2} (a.u)	I_{S3} (a.u)	I_{S4} (a.u)	I_{S5} (a.u)	I_{S6} (a.u)	I_{S7} (a.u)	I_{S8} (a.u)
Ni I	222.29	167.36	167.62	167.48	167.52	167.74	167.39	167.20	167.52
	336.57	----	----	----	----	----	----	----	----
Ni II	227.8	----	----	----	----	----	----	----	----
As I	234.98	167.25	167.10	167.31	167.41	167.14	167.10	167.08	167.14
As II	225.31	----	----	----	----	----	----	----	----
Ru I	300.55	167.59	----	----	167.42	----	----	----	167.69
Th I	378.91	167.87	168.42	167.80	167.43	167.97	168.65	167.87	167.96
	436.59	167.38	167.91	----	----	----	----	----	----
	451.05	170.14	----	----	----	----	----	----	----
Th II	299.06	167.62	167.28	167.54	----	167.78	167.70	167.81	167.70
	635.90	----	----	----	----	----	----	----	----
Th III	358.28	----	----	----	----	----	----	167.33	167.40
Zr I	457.55	----	167.60	167.24	167.48	167.52	167.40	167.79	167.43
Zr II	738.28	----	----	----	----	----	----	----	----
Tb I	470.24	167.17	167.09	170.21	167.20	167.40	167.03	167.16	167.33
Eu I	537.69	----	----	----	----	----	----	----	----
Li I	548.51	167.51	167.51	----	167.64	167.73	167.42	167.59	167.43
I I	562.56	168.40	----	----	----	----	----	----	----
Cu I	615.03	168.11	167.40	167.18	168.03	167.47	167.52	167.69	167.90
Xe I	627.75	167.68	167.42	167.96	167.57	167.69	167.87	167.57	168.07
K I	693.87	-----	167.92	167.91	167.98	167.60	----	170.24	167.41
	534.29	167.83	167.91	170.21	168.64	168.82	168.74	170.26	167.63
He I	706.57	167.22	167.38	167.38	167.38	167.55	167.34	167.60	167.87
Ne I	772.46	167.54	167.20	167.51	167.46	167.83	167.64	167.62	168.06
Cs I	782.25	167.32	167.57	167.57	167.80	167.99	167.59	167.87	167.80
Cs II	358.28	----	----	----	----	----	----	167.33	167.40
Cs III	353.30	----	----	----	----	----	----	----	----
Hg I	313.18	167.19	167.54	167.93	167.22	167.36	167.40	167.46	----
Cr I	391.62	167.20	167.49	167.62	167.40	167.55	167.81	167.59	167.56
Cr II	353.20	----	----	----	----	----	----	----	----
Cr III	204.84	----	----	----	----	----	----	----	----
Cu I	615..0 3	168.11	167.40	167.57	168.05	167.47	167.82	167.69	168.91
Na I	654.77	167.20	----	168..08	168.09	167.30	----	----	167. 96
Fe I	370.79	167.87	168.42	167.43	----	167.97	168.39	167.87	----
Fe II	369.84	----	170.26	----	167.20	----	----	----	----
Fe III	208.59 227.81 492.65	----	----	----	----	----	----	----	----

Tl I	307.29	----	----	----	----	----	----	----	----
Tl II	213.75	-----	----	----	----	-----	----	----	----
Tl III	391.56	167.20	167.49	167.62	167.40	167.56	167.44	167.59	167.56

4.2.3 Irradiation by 100 mJ:

When the pulse energy was increased to 100mj, some ions were appeared in the sample spectra at higher order ofionization stages, like: Cr III, Tl III, and Fe II.Figures from (4-17) to (4-24) and table (4-3) illustrated that fact.

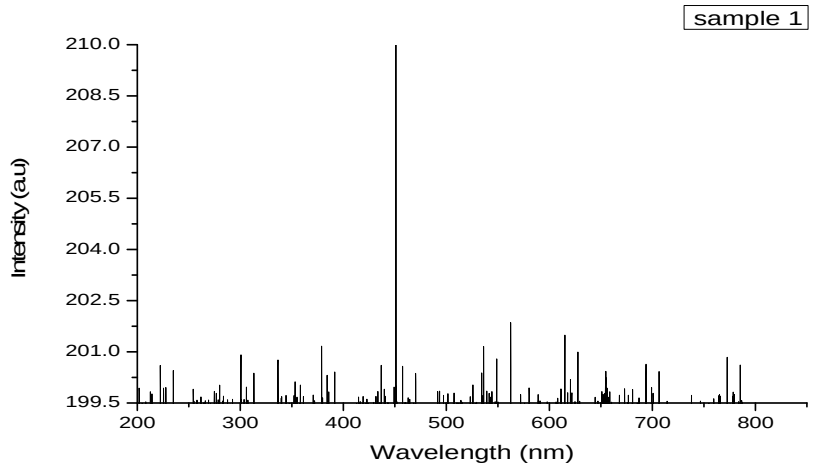

Fig(4-17) LIBS emission spectrum of sample1 after irradiation by100 mJ.

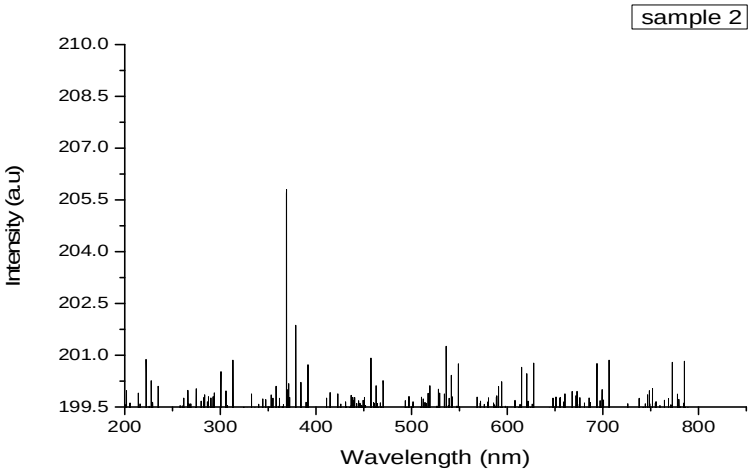

Fig(4-18) LIBS emission spectrum of sample2 after irradiation by 100 mJ.

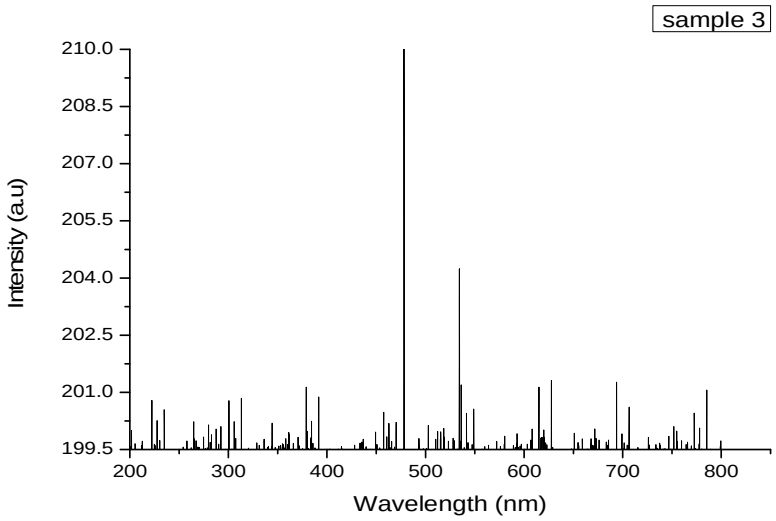

Fig(4-19) LIBS emission spectrum of sample3 after irradiation by 100 mJ.

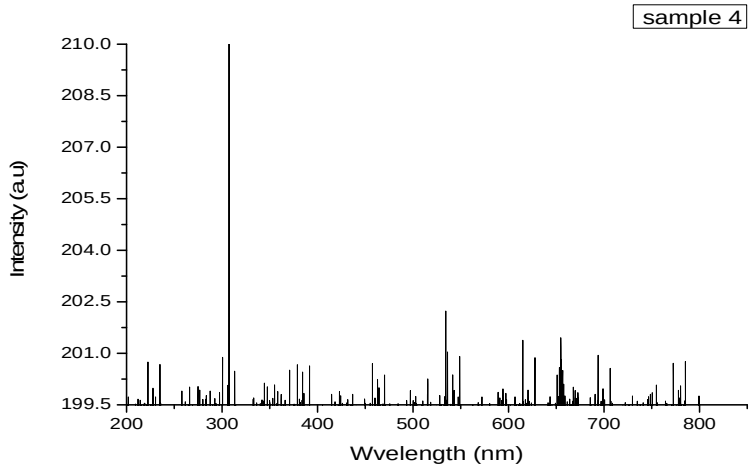

Fig(4-20) LIBS emission spectrum of sample4 after irradiation by 100 mJ.

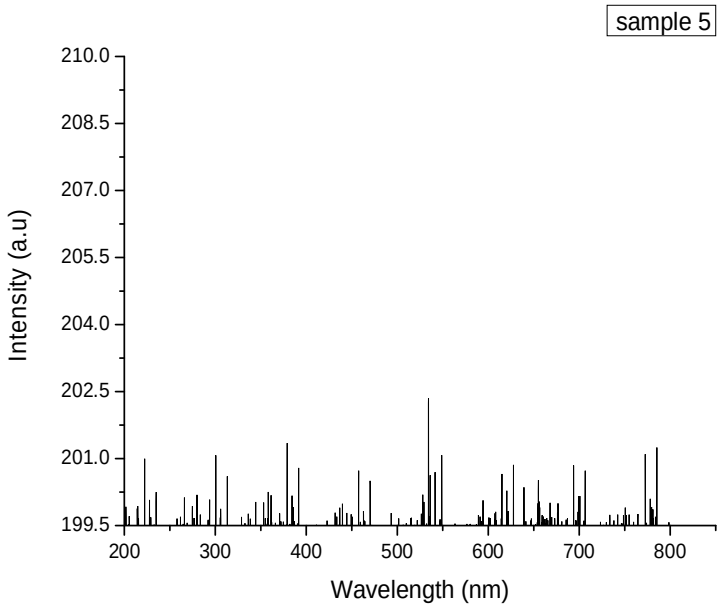

Fig(4-21) LIBS emission spectrum of sample5 after irradiation by 100 mJ.

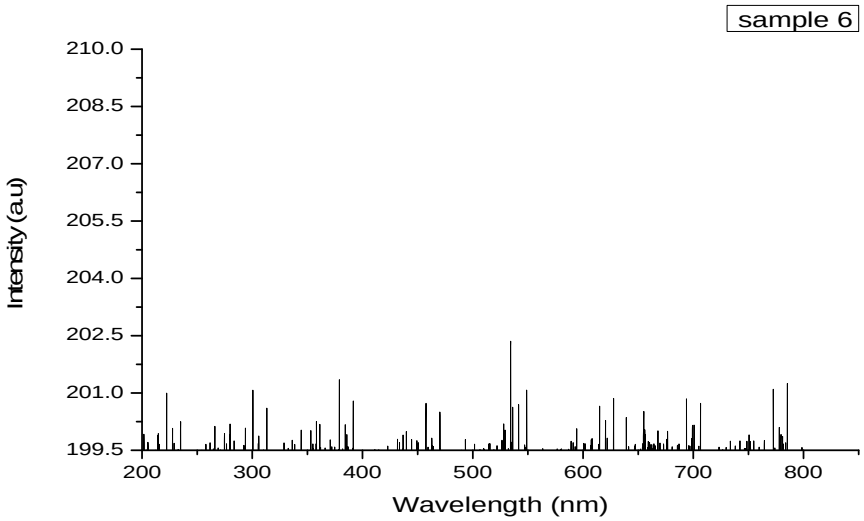

Fig(4-22) LIBS emission spectrum of sample6 after irradiation by 100 mJ.

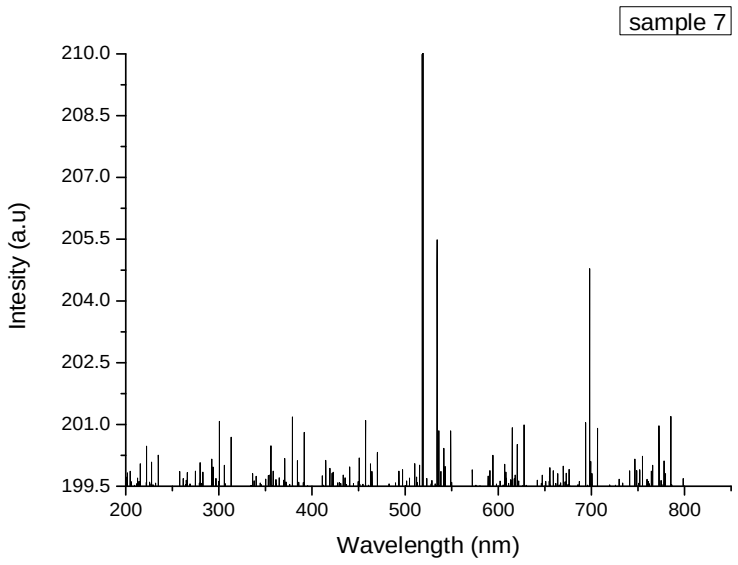

Fig(4-23) LIBS emission spectrum of sample7 after irradiation by 100 mJ.

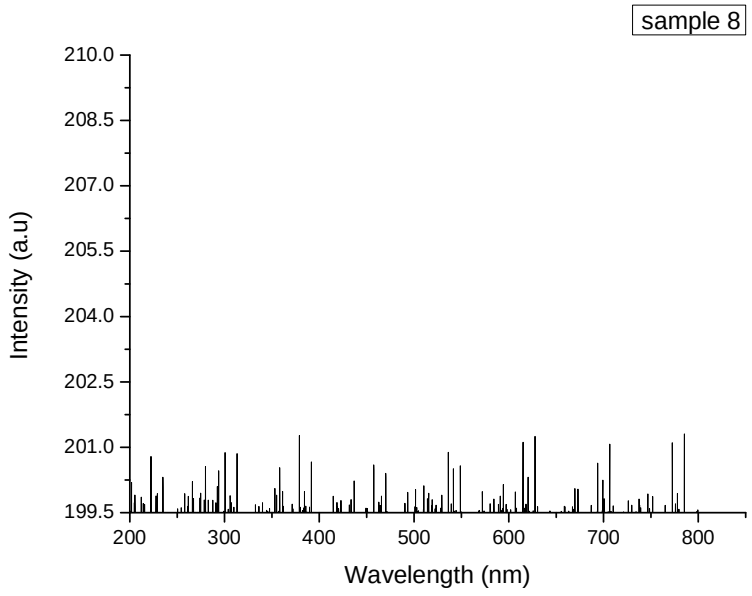

Fig(4-24) LIBS emission spectrum of sample8 after irradiation by 100 mJ.

Table (4-3) the analyzed data of the eight samples after irradiation by 100mJ:

Element	λ (nm)	I_{S1} (a.u)	I_{S2} (a.u)	I_{S3} (a.u)	I_{S4} (a.u)	I_{S5} (a.u)	I_{S6} (a.u)	I_{S7} (a.u)	I_{S8} (a.u)
Ni I	222.29 336.57	201.19 ------	201.57 -----	201.29 ----	201.93	201.52 -----	201.67 ----	201.04 ----	201.38 ----
Ni II	227.8	------	-----	----	-----	-----	----	----	----
As I	234.98	201.14	200.76	201.19	201.33	200.90	201.00	201.28	201.33
As II	225.31	------	-----	-----	-----	-----	----	----	----
Ru I	300.55	------	-----	-----	-----	-----	-----	----	----
Th I	378.91 436.59 451.05	201.91 201.28 210.78	202.51 ------ ------	201.81 ------ ------	-----	201.96 ---- ----	-----	202.24 ---- 202.12	202.30 ---- ----
Th II	299.06 635.90	201.43 ------	201.14 -----	201.87 -----	201.52	201.62 -----	---- ----	202.00 ----	201.86 ----
Th III	358.28	------	-----	-----	-----	-----	----	----	----
Zr I	457.55	201.24	201.67	201.14	201.43	201.33	201.38	201.12	201.14
Zr II	738.28	------	-----	-----	-----	-----	----	----	----
Tb I	470.24	200.95	201	-----	201.09	200.95	201.14	201.28	200.90
Eu I	537.69	201.86	-----	-----	----	202.92	-----	----	----
Li I	548.51	201.53	-----	201.29	201.57	201.67	201.67	201.43	201.57
I I	562.56	202.34	-----	-----	-----	----	----	----	----
Cu I	615.03	202.15	201.32	201.72	202	201.24	201.28	201.62	201.67
Xe I	627.75	201.67	201.43	201.96	201.52	201.43	201.48	201.94	202.07
K I	693.87 534.29	201.38 -----	201.38 201.96	201.86 204.83	201.57 202.87	201.43 202.94	201.93 203.13	205.36 206.13	201.48 201.50
He I	706.57	201.24	201.53	201.52	201.24	201.33	202.31	201.48	201.63
Ne I	772.46	201.53	201.43	201.09	201.38	201.71	202.59	201.67	201.76
Cs I	782.25	201.28	201.33	201.72	201.24	201.96	202.55	202.11	201.86
Cs II	358.28	------	----	-----	-----	-----	----	----	----
Cs III	353.30	------	----	-----	-----	-----	----	----	----
Hg I	313.18	201.01	201.38	201.52	-----	201.28	201.19	201.72	201.86
Cr I	391.62	201.05	201.48	200.92	201.28	201.33	201.33	201.92	201.74
Cr II	353.20	-----	-----	-----	-----	----	----	201.52	----
Cr III	204.84	-----	-----	-----	-----	----	----	----	----
Cu I	615..0 3	201.15	201.33	201.72	201.91	201.24	201.28	201.62	201. 67
Na I	654.77	201.16	-----	-----	202.05	201.93	202.07	----	----
Fe I	370.79	------	-----	----	-----	----	----	---	----
Fe II	369.84	------	-----	-----	201.09	----	----	-----	----
Fe III	208.59 227.81 492.65	-----	-----	-----	-----	----	----	----	----

Tl I	307.29	-----	-----	-----	210.87	----	----	----	----
Tl II	213.75	-----	-----	-----	-----	----	----	----	----
Tl III	391.56	-----	201.48	201.52	201.28	201.33	201.35	201.92	201.74

4.2.4 Irradiation by 120 mJ:

After increasing the laser pulse to 120mJ, some ions were appeared at higher order of ionization stages, like CsII, Tl III, Cs III andZr II .Figures from (4-25) to (4-32) and table (4-4) illustrated that fact.

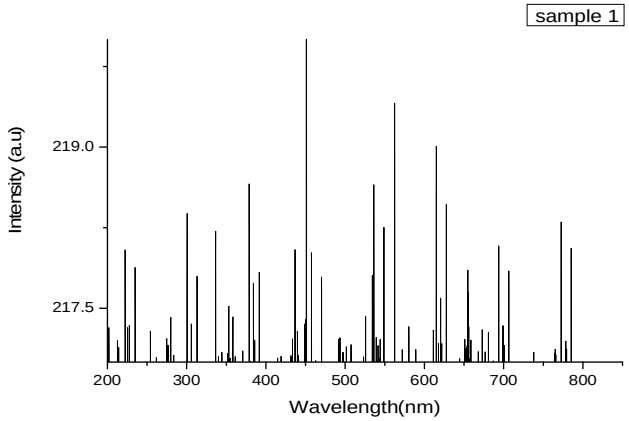

Fig(4-25) LIBS emission spectrum of sample1 after irradiation by 120 mJ.

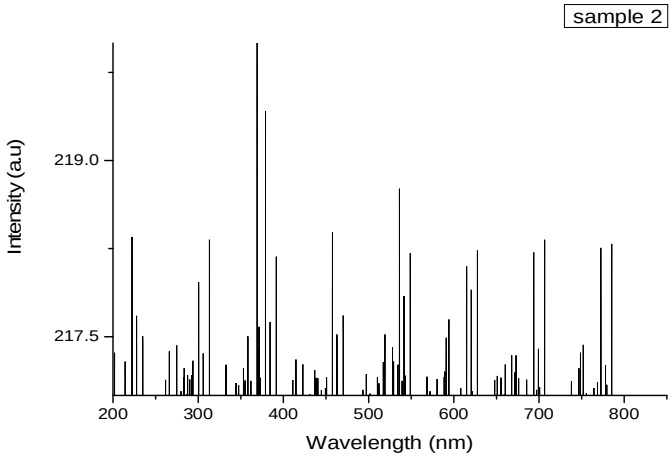

Fig(4-26) LIBS emission spectrum of sample2 after irradiation by 120 mJ.

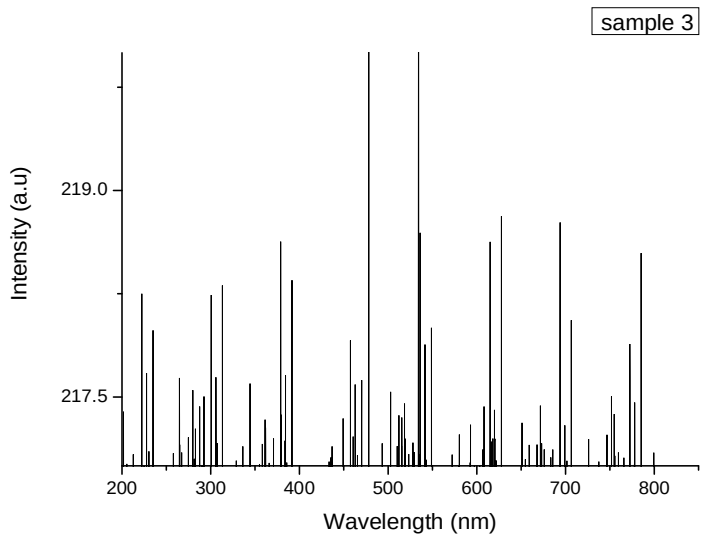

Fig(4-27) LIBS emission spectrum of sample3 after irradiation by 120mJ.

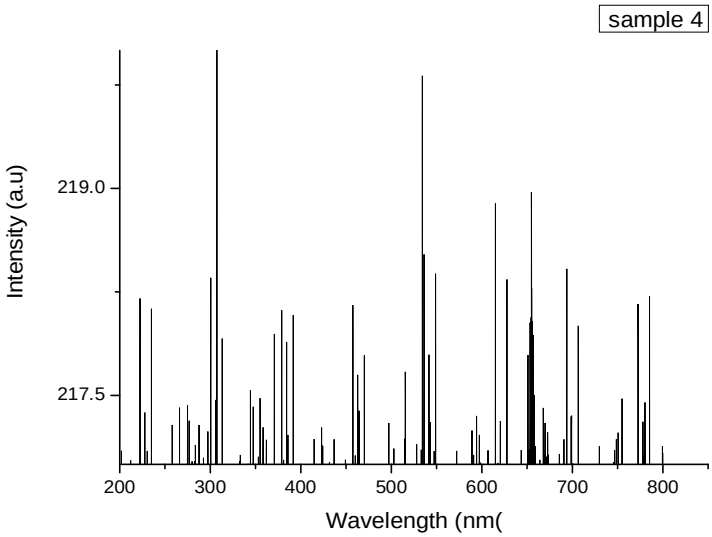

Fig (4-27) LIBS emission spectrum of sample 4 after irradiation by 120 mJ.

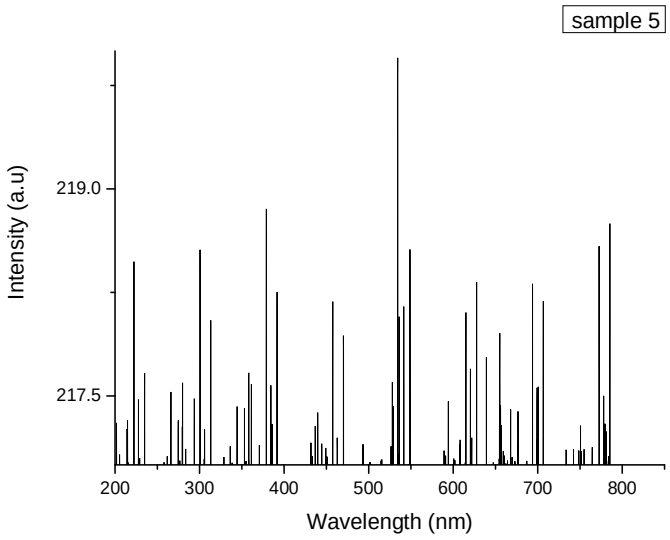

Fig(4-29) LIBS emission spectrum of sample5 after irradiation by 100 mJ.

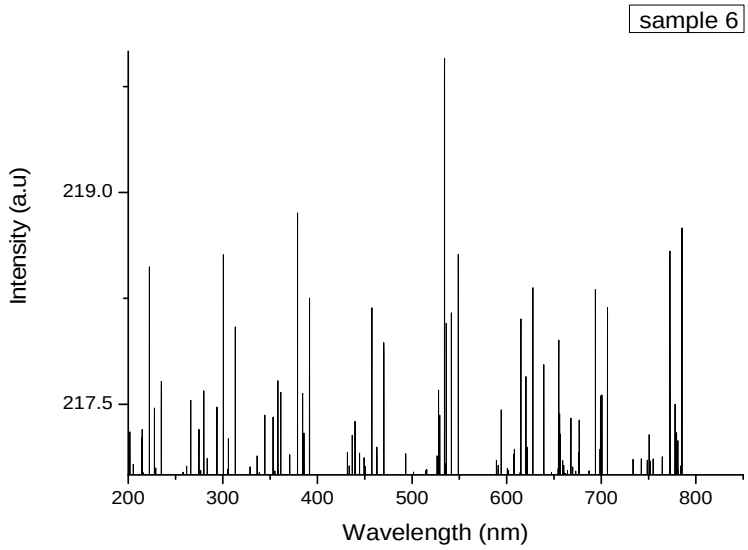

Fig(4-30) LIBS emission spectrum of sample6 after irradiation by 120 mJ.

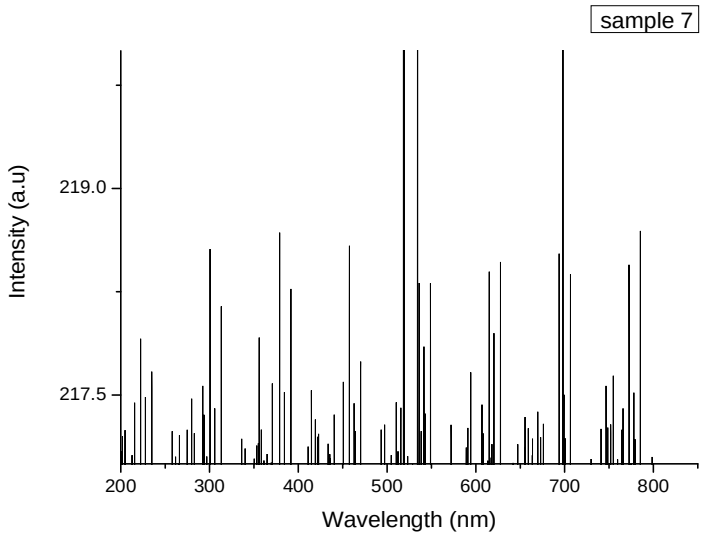

Fig(4-31) LIBS emission spectrum of sample7 after irradiation by 120 mJ.

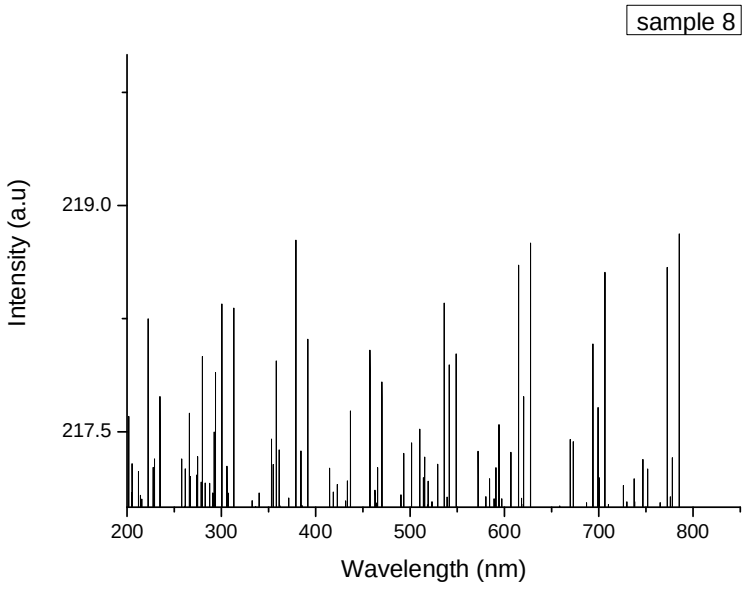

Fig(4-32) LIBS emission spectrum of sample8 after irradiation by 120 mJ.

Table (4-4): the analyzed data of the eight samples after irradiation by120 mJ.

Element	λ (nm)	I_{S1} (a.u)	I_{S2} (a.u)	I_{S3} (a.u)	I_{S4} (a.u)	I_{S5} (a.u)	I_{S6} (a.u)	I_{S7} (a.u)	I_{S8} (a.u)
Ni I	222.29 336.57	218.27 ------	218.49 -----	218.55 ----	218.38	218.36 ------	218.71 -----	218.70 ----	218.42 -----
Ni II	227.8	------	-----	----	-----	------	-----	----	-----
As I	234.98	218.20	217.80	218.14	218.30	217.82	217.82	218.85	218.90
As II	225.31	------	-----	-----	-----	------	-----	-----	-----
Ru I	300.55	218.57	-----	-----	-----	-----	-----	-----	-----
Th I	378.91 436.59 451.05	218.84 218.15 220.16	219.59 ------ ------	218.77 ------ ------	218.27 -----	219.01 ----- -----	219.09 ------ ------	218.84 ------ 217.77	218.92 -----
Th II	299.06 635.90	----- 218.83	219.14 -----	201.87 -----	218.49 -----	218.73 217.93	219.14 -----	218.87 -----	218.48 -----
Th III	358.28	------	-----	-----	-----	------	-----	218.08	218.19
Zr I	457.55	218.28	218.55	218.41	218.32	218.30	218.17	218.73	218.22
Zr II	738.28	218.84	-----	-----	-----	----	-----	-----	-----
Tb I	470.24	218.07	217.84	-----	217.97	218.10	218.00	217.95	218.03
Eu I	537.69	218.83	-----	-----	----	-----	-----	-----	----
Li I	548.51	218.55	218.40	218.16	218.55	218.72	-----	218.48	218.22
I I	562.56	219.58	-----	-----	-----	-----	-----	-----	-----
Cu I	615.03	219.18	218.26	218.78	219.05	218.27	218.26	218.55	218.77
Xe I	627.75	218.67	218.41	219.00	218.49	218.51	218.49	218.66	218.96
K I	693.87 534.29	218.64 218.83	218.39 218.92	218.92 220.18	218.58 219.90	218.42 220.11	218.41 220.10	220.16 220.20	218.23 218.51
He I	706.57	218.06	218.48	218.22	218.16	218.36	218.48	218.53	218.74
Ne I	772.46	218.49	218.44	218.05	218.36	218.74	218.44	218.62	218.75
Cs I	782.25	218.28	218.47	218.70	218.36	218.92	218.37	218.85	218.97
Cs II	358.28	------	----	-----	-----	217.82	217.92	218.73	218.91
Cs III	353.30	217.73	----	-----	-----	-----	----	-----	-----
Hg I	313.18	217.93	218.52	218.48	218.17	218.93	218.23	218.31	218.17
Cr I	391.62	218.04	218.36	218.53	218.27	218.42	218.44	218.49	218.27
Cr II	353.20	217.70	-----	-----	-----	-----	-----	-----	-----
Cr III	204.84	-----	-----	-----	-----	-----	-----	-----	-----
Cu I	615.03	219.18	218.26	218.78	219.00	218.27	218.28	218.55	218.66
Na I	654.77	218.05	-----	-----	219.12	218.10	-----	-----	-----
Fe I	370.79	------	219.59	218.77	218.97	------	-----	-----	-----
Fe II	369.84	------	220.18	-----	-----	------	----	-----	-----
Fe III	208.59 227.81 492.65	-----	-----	-----	-----	-----	-----	-----	-----

Tl I	307.29	-----	-----	-----	210.87	-----	-----	-----	-----
Tl II	213.75	-----	-----	-----	-----	-----	-----	-----	-----
Tl III	391.56	218.04	218.36	218.53	218.27	218.42	218.45	218.49	218.30

4.3 Discussion:

The eight samples wereirradiated by pulse laser energy 60 mJ, and the spectra of these samples were recorded as shown in figures (4-1) to (4-8).The recorded spectra were analyzed and the identification of the spectral lines arelisted in table (4-1). This table illustrate that the atoms were excited to higher energy states.

The eight spectra of the samples showed different types with different amounts, include heavy elements like (Ni, As, Ru, Th, Zr, Tb, Eu, Cu, Xe, Cs, Hg, Cr, Tl, Cu, Ra and Fe) that were found in all samples with different irradiated pulse energy.

It is clear from table (4-1), that the Ironatoms were appeared in sample (4,5,6,7,8) and disappeared in samples (1,2,3) due to the location of the sample. Iron ions were appeared in higher ionization states because the laser energy was sufficient to excite this metal in samples (1, 2, 3, 4, 8).

Thallium atoms were appeared in samples (4,7)with higher amount especially in sample (4), also Thallium ions were appeared in samples (1,2,3,4,7,8) with higher amount in sample (7).

Chromium atoms were found at different amounts and excited with low pulse energy in samples (2, 3, 4, 5, 6, 7, 8). Chromium is toxic metal even with little amount.

Mercury atoms (Hg) were found with relatively little amount in all samples except sample (1),this element is highly toxic even with little amount.

Beside neutral atoms, ions with different amounts and ionization stages also were recorded as shown in Table (4-1). All these ions may not present in the

sample originally, where some of them are produced due to the ionization of neutral atoms by the laser power density.

The pulse energy was increased to 80 mJ and the spectra of the eight samples were recorded in the same region as shown in figures (4-9) to (4-16).The recorded spectra were analyzed and the spectral lines are listed in table (4-2).The emission intensity of the metals were increased compared with the case of 60 mJ.

This table illustrates that the number of atoms in the excited state was increased, this is due to increasing the pulse energy.

Increasing of pulse energy to 80 mJ increased the amount of Cesium atoms in all eight samples. Cesium ion (Cs^{+1}) was presented with relatively little amount in samples (7, 8) and disappeared in other samples. Also Iron ions (Fe^{+1}) was found with low amount in samples (2, 4).The Thorium ions (Th^{+2}) were found with relatively low amount in all samples except sample (4).

The Thallium ions (Tl^{+2}) were foundwith low amountin all samples.The Zirconium atoms (Zr) were found in relatively equal amount in all samples even sample (1) and the Zirconium ions (Zr^{+1}) werenot found in all samples.

Beside neutral atoms, ions with different amounts and ionization stages were recorded as shown in tables (4-1) to table (4-4). All these ions may not presented in the samples originally, where some of them are produced due to the ionization of neutral atoms by the laser power density.

The pulse energy was increased to 100 mJ and the spectra of the eight samples were recorded in the same region as shown in figures (4-17) to (4-24).The recorded spectra were analyzed and the spectral lines are listed in table (4-3). Sample (1) had large amount of metals, most of ions were appeared at different ionization stages by the laser power density.

Thallium atoms (Tl) were appeared with relatively high amount in sample (4) only butThallium ions (Tl^{+2}) were appearedwith relatively low amount in all samples even sample (1).Chromium atoms (Cr) were appeared in all samples with nearly amount,and (Cr^{+1}) were found with low amount in sample (7) only due to the pulse energy.

Cesium atoms (Cs) were presented in all samples with different amounts but the ions of it weren't appear in any sample.Mercury (Hg)atoms were appeared inall samples except sample (4) with nearly amount. The ions ofFe^{+1}were appeared only in sample (4).

Ti atoms werefound only in sample (4), and (Ti^{+2})ions were appeared in samples (2, 3, 4,5,6,7 and 8) with different amount.

When the laser energy was increased to 120 mj, Ni atoms were appeared in all samples. Also (Th,Zr, Hg, Cr, As) atomswere appeared in all samples with nearly equal amounts.

Th^{+1}ions were presented with high amount in samples (2,6) and relatively in high amount in other samples.

Fe atoms were appeared in samples (1, 2,3) with high amount.Fe^{+1}ionswere appeared in sample (2) only with high amount.

From these results it is clear that: the amount of different atoms and ions were appeared in all eight samples and their spectral intensities depend on the power density of the laser. Also the ionization of neutral atoms depends on the laser power density.

Figures (4-1) to (4-32) showed the plot of the intensity at laser pulse energy 60, and 80, 100, 120 mJ, via wavelengths of the appeared metals found in the eight samples. Intensity here is the number of atoms per unit volume.

Intensity was decreased by increasing the pulse energy some of atoms were appeared as ions at different ionization stages, this lead to decreasing the emitted intensity of them.

Some heavy metals like: (Fe, Hg, Cr, Tl and Mn) with high atomic weight were appeared in the eight water samples with different amounts. While (Cr, Hg, and Tl) were appeared in the eight samples with nearly amount, they are toxic metals, harmful to human and environment.Also metals like: (Na, I, Cu and K) with small atomic weight were appeared in many water samples with different amounts.

4. 4 Conclusions:

From the obtained results one can conclude that:

1. The analysis of the water samples using LIBS technique led to the determination of different heavy metals.
2. Cr and Hg atoms were appeared in all samples with different concentrations at different pulse energies, these metals are highly toxic.
3. This study reveals that the water samples, collected from different places in Khartoum State, are contaminated by several toxic elements like: Titanium, chromium, and Mercury. Most of these elements are considered as highly toxic and carcinogens. They could cause a lot of problems to human like heart and lungs deceases.

4. 5 Recommendations:

The followings can be recommended as future work:

1. There is a need to establish a correlation between the used power density and the ionization energy of each heavy element.
2. Double pulse lasers can be used to enhance the detected signal.

3. The LIBS system can be used as a portable system for on line analysis of water inany place. Investigations should be made to reduce the size and the initial cost of the instrumentation.
4. It is better to use evacuation system to get more accurate results.
5. It is better to use delay time system to control and uniform the measurements instead of manually capturing the spectra.
6. LIBS can be used for the determination of elements concentration in each sample.

References:

Anderson, D.M.W. and Herbich, M.A., (1963), 1.Studies on uronic acid materials. Part VI. The variation in composition and properties of gum nodules from Acacia seyal del. *Journal of the Chemical Society (Resumed)*: pp.1-6.

DAVID, A.C. and RADZIEMSKI, L.J., (2006), Handbook of laser-induced breakdown spectroscopy.*Cambridge University*, *25*.
De Lucia, F.C. and Gottfried, J.L., (2011), Influence of variable selection on partial least squares discriminant analysis models for explosive residue classification. *SpectrochimicaActa Part B: Atomic Spectroscopy*, ***66***(2): pp.122-128.

Federer, H., (2014), *Geometric measure theory*. Springer.Fan, H., Shi, Q., Yan, H., Ji, S., Dong, J. and Zhang, G., (2014), Simultaneous Spray Self-Assembly of Highly Loaded ZIF-8–PDMS Nanohybrid Membranes Exhibiting Exceptionally High Biobutanol-PermselectivePervaporation.*AngewandteChemie International Edition*, ***53***(22): pp.5578-5582.

Fichet, P., Mauchien, P., Wagner, J.F. and Moulin, C., (2001), Quantitative elemental determination in water and oil by laser induced breakdown spectroscopy. *Analyticachimicaacta*, ***429***(2): pp.269-278.

Franz Mayinger, (1994), Optical Measurements, springer- Verlag Germany.

F.C. DeLuciaJr, J.L. Gottfried, Mater, (2011).
Gornushkin, S.I., Gornushkin, I.B., Anzano, J.M., Smith, B.W. and Winefordner, J.D, (2002), Effective normalization technique for correction of matrix effects in laser-induced breakdown spectroscopy detection of magnesium in powdered samples.*Applied spectroscopy*, ***56***(4): pp.433-436.

Gilbarg, D. and Trudinger, N.S., (2015), *Elliptic partial differential equations of second order*.springer.
Gu, X. and Yau, S.T., (2003), June. Global conformal surface parameterization.In *Proceedings of the 2003 Eurographics/ACM SIGGRAPH symposium on Geometry processing* (pp. 127-137).Eurographics Association.

Gaudiuso, R., Dell'Aglio, M., Pascale, O.D., Senesi, G.S. and Giacomo, A.D., (2010).Laser induced breakdown spectroscopy for elemental analysis in environmental, cultural heritage and space applications: a review of methods and results. *Sensors*, ***10***(8): pp.7434-7468.

Hollas, J.M.,(2004),*Modern spectroscopy*. John Wiley & Sons.

Hodnett, P.A. and Ko, J.P., (2012),Evaluation and management of indeterminate pulmonary nodules. *Radiologic Clinics of North America*, ***50***(5): pp.895-914.

Hammer, S.M., Saag, M.S., Schechter, M., Montaner, J.S., Schooley, R.T., Jacobsen, D.M., Thompson, M.A., Carpenter, C.C., Fischl, M.A.,

Gazzard, B.G. and Gatell, J.M., (2006), Treatment for adult HIV infection: 2006 recommendations of the International AIDS Society–USA panel. *Jama*, ***296***(7): pp.827-843.

Jenkins, H., Purushotma, R., Weigel, M., Clinton, K. and Robison, A.J., (2009), *Confronting the challenges of participatory culture: Media education for the 21st century*. Mit Press.

Larkins, P. and Payling, R., (2000),*Optical Emission Lines of the Elements: CD-ROM*. Wiley.

Li, H., Su, W., Wang, C.Y. and Huang, Z., 2009. Ambient noise Rayleigh wave tomography in western Sichuan and eastern Tibet. *Earth and Planetary Science Letters*, ***282***(1):pp.201-211.

Lui, S.L., Godwal, Y., Taschuk, M.T., Tsui, Y.Y. and Fedosejevs, R., (2008), Detection of lead in water using laser-induced breakdown spectroscopy and laser-induced fluorescence.*Analytical Chemistry*, ***80***(6): pp.1995-2000.

Lönnroth, K., Jaramillo, E., Williams, B.G., Dye, C. and Raviglione, M., (2009), Drivers of tuberculosis epidemics: the role of risk factors and social determinants. *Social science & medicine*, ***68***(12): pp.2240-2246.

Milonni, P.W. and Eberly, J.H., (2010),Laser Physics.

McCreery, R.L., (2005),*Raman spectroscopy for chemical analysis* (Vol. 225). John Wiley & Sons.

Michel, A.P., Lawrence-Snyder, M., Angel, S.M. and Chave, A.D., (2007), Laser-induced breakdown spectroscopy of bulk aqueous solutions at oceanic pressures: evaluation of key measurement parameters. *Applied optics*, ***46***(13): pp.2507-2515.

Maeda, K., Kobayashi, Y., Udagawa, N., Uehara, S., Ishihara, A., Mizoguchi, T., Kikuchi, Y., Takada, I., Kato, S., Kani, S. and Nishita,

M., (2012), Wnt5a-Ror2 signaling between osteoblast-lineage cells and osteoclast precursors enhances osteoclastogenesis. *Nature medicine*, ***18***(3): pp.405-412.

Ogura, Y., Bonen, D.K., Inohara, N., Nicolae, D.L., Chen, F.F., Ramos, R., Britton, H., Moran, T., Karaliuskas, R., Duerr, R.H. and Achkar, J.P., (2001),A frameshift mutation in NOD2 associated with susceptibility to Crohn's disease. *Nature*, ***411***(6837): pp.603-606.

OrazioSvelto Translated from Italian and edited by David C. Hanna, (1998), Principles of Lasers, 4th ed., springer- Verlag Germany.

Peichao, Z., Hongdi, L., Jinmei, W., Bin, Y., Rui, Y., Bin, Z. and Xiaomeng, W., (2014), Study on time evolution process of laser-induced aluminum alloy plasma. *Chinese J Lasers*, ***41***(10): p.1015001.

Palleschi, A. Salvetti, E. Tognoni,Spectrochim. Acta, (2002), Part B 57, 339.

Renard, D., Lavenant-Gourgeon, L., Ralet, M.C. and Sanchez, C., (2006),Acacia s enegal Gum: Continuum of Molecular Species Differing by Their Protein to Sugar Ratio, Molecular Weight, and Charges. *Biomacromolecules*, ***7***(9): pp.2637-2649.

Ryan, R.M. and Deci, E.L., (2000), Self-determination theory and the facilitation of intrinsic motivation, social development, and well-being.*American psychologist*, ***55***(1): p.68.

Radziemski, L.J. and Cremers, D.A.,(2006), Handbook of Laser Induced Breakdown Spectroscopy

Radziemski, L.J., (2002), From LASER to LIBS, the path of technology development. *SpectrochimicaActa Part B: Atomic Spectroscopy*, ***57***(7):pp.1109-1113.

Rai, A.K., (2002), Specialized Trial Courts: Concentrating Expertise on Fact. *Berkeley Technology Law Journal*:pp.877-897.

Renard, D., Lavenant-Gourgeon, L., Ralet, M.C. and Sanchez, C., 2006. Acacia s enegal Gum: Continuum of Molecular Species Differing by Their Protein to Sugar Ratio, *Molecular Weight, and Charges. Biomacromolecules, 7(9), pp.2637-2649*

Smith, E. and Dent, G., (2005), Introduction, basic theory and principles.*Modern Raman spectroscopy-A practical approach*: pp.1-21.

Singh, J.P. and Thakur, S.N. eds.,(2007), *Laser-induced breakdown spectroscopy*. Elsevier.

Sirin, E., Parsia, B., Grau, B.C., Kalyanpur, A. and Katz, Y., (2007), Pellet: A practical owl-dl reasoner. *Web Semantics: science, services and agents on the World Wide Web*, ***5***(2): pp.51-53.

Shaw, J.E., Sicree, R.A. and Zimmet, P.Z., (2010), Global estimates of the prevalence of diabetes for 2010 and 2030.*Diabetes research and clinical practice*, ***87***(1): pp.4-14.

Shunchun, Y., Jidong, L. and Shenghua, P., (2010), Analysis of unburned carbon in coal fly ash by using laser-induced breakdown spectroscopy in deep UV.*Chinese J. Lasers*, ***37***(4): pp.1114-1117.

Svelto, O., (2010), Properties of laser beams.In *Principles of Lasers* (pp. 475-504).Springer US.

Singh, J.P. and Thakur, S.N. eds., (2007), *Laser-induced breakdown spectroscopy*.Elsevier.

Tsuji, J., (2006), *Palladium reagents and catalysts: new perspectives for the 21st century*. John Wiley & Sons.

Yaroshchyk, P., Death, D.L. and Spencer, S.J., (2010), Quantitative measurements of loss on ignition in iron ore using laser-induced breakdown spectroscopy and partial least squares regression analysis. *Applied spectroscopy*, ***64***(12):pp.1335-1341.

Zhang, S., Eitel, R.E., Randall, C.A., Shrout, T.R. and Alberta, E.F., (2005), Manganese-modified BiScO3-PbTiO3 piezoelectric ceramic for high-temperature shear mode sensor. *Applied Physics Letters*, ***86***(26): pp.262904-262904om.